**UNIVERSITY OF PARDUBICE**

**FACULTY OF CHEMICAL TECHNOLOGY**

# THESIS

**2024** **MSc. NICHOLAS EBUKOLO**

**UNIVERSITY OF PARDUBICE**

**FACULTY OF CHEMICAL TECHNOLOGY**

INSTITUTE OF APPLIED PHYSICS AND MATHEMATICS

# SELF-CROSSLINKING FILM-FORMING LATEXES PREPARED USING SUNFLOWER OIL-BASED MONOMER

Master Thesis

2024 MSc. Nicholas Ebukolo

University of Pardubice
Faculty of Chemical Technology
Academic year: 2023/2024

# ASSIGNMENT OF DIPLOMA THESIS

**(project, art work, art performance)**

| | |
|---|---|
| Name and surname: | **MSc. Nicholas Ebukolo** |
| Personal number: | **C22173** |
| Study programme: | **N0531A130032 Materials Chemistry** |
| **Work topic:** | **Self-crosslinking film-forming latexes prepared using sunflower oil--based monomer** |
| Assigning department: | **Institute of Applied Physics and Mathematics** |

## Theses guidelines

1. Prepare a literature survey related to the given topic. 2. Prepare two series of latexes differing in the type of anionic emulsifier (non-polymerizable vs. polymerizable) via emulsion polymerization. Use an acrylated derivative of sunflower oil, styrene, butyl acrylate, diacetone acrylamide, and methacrylicacid as starting monomers. To ensure "self-crosslinking", add an appropriate amount of adipic acid dihydrazide to the latexes after the synthesis is complete. 3. Evaluate the basic properties of the pre- pared latexes (coagulum content, particle size, minimum film-forming temperature, storage stability).

4. Make coating films and assess their properties concerning the content of the bio-monomer and the type of emulsifier used. Also, focus on the surface properties of the coatings and their water sensitivity.
5. Process the obtained information clearly in the form of a diploma thesis following the UPa Directive No. 7/2019 "Rules for submission, publication and formal preparation of theses" as amended.

**Extent of work report:**

Extent of graphics content:

**Form processing of diploma thesis: printed**

Language of elaboration: **English**

**Recommended resources:**

scientific articles from the relevant literature

Supervisors of diploma thesis: **doc. Ing. Jana Machotová, Ph.D.**

**Institute of Chemistry and Technology ofMacromolecular Material**

Date of assignment of diploma thesis: **February 29, 2024**

Submission deadline of diploma thesis: **May 3, 2024**

L.S.

**prof. Ing. Petr Němec, Ph.D.**

Dean

**prof. Ing. Čestmír Drašar, Dr.**

Head of Department

In Pardubice February 29, 2024

I declare:

The thesis entitled Self-crosslinking film-forming latexes prepared using sunflower oil-based monomer is my own work. All literary sources and information I used in the thesis are referenced in the bibliography. I have been acquainted with the fact that my work is subject to the rights and obligations arising from Act No. 121/2000 Sb., On Copyright, on Rights Related to Copyright and on Amendments to Certain Acts (Copyright Act), as amended, especially with the fact that the University of Pardubice has the right to conclude a license agreement for the use of this thesis as a school work under Section 60, Subsection 1 of the Copyright Act, and that if this thesis is used by me or a license to use it is granted to another entity, the University of Pardubice is entitled to request a reasonable fee from me to cover the costs incurred for the creation of the work, depending on the circumstances up to their actual amount.

I acknowledge that in accordance with Section 47b of Act No. 111/1998 Sb., On Higher Education Institutions and on Amendments to Other Acts (Act on Higher Education Institutions), as amended, and the Directive of the University of Pardubice No. 7/2019 Rules for Submission, Publication and Layout of Theses, as amended, the thesis will be published through the Digital Library of the University of Pardubice.

In Pardubice on 10 May 2024

MSc. Nicholas Ebukolo

The diploma thesis was created with the support of the project Modernization of practical teaching and improvement of practical skills in technically oriented study programs, reg. number CZ.02.2.67/0.0/0.0/16_016/0002458 of the operational program Research, development, and education. This project is co-financed by the European Union.

EVROPSKÁ UNIE
Evropské strukturální a investiční fondy
Operační program Výzkum, vývoj a vzdělávání

MINISTERSTVO ŠKOLSTVÍ,
MLÁDEŽE A TĚLOVÝCHOVY

# ACKNOWLEDGMENT

First and foremost, praises and thanks to God, the Almighty, for the strength and showers of blessings throughout my research work.

I would like to express my deep and sincere gratitude to my research supervisor, Mrs. doc. Ing. Jana Machotová, Ph.D., for giving me the opportunity to do this research under her supervision. She provided me with invaluable professional guidance, help, patience, willingness, and great support during the writing of this thesis and during my laboratory work. It was a great privilege and honor to work under her guidance.

I am extremely grateful to my programme coordinator doc. RNDr. Petr Janíček, Ph.D., for his love, friendship, empathy, sacrifices, and guidance towards completing the research work and the study programme. I am grateful for what he has offered me.

I would also like to thank Mrs. Dagmar Pitthardová for practical advice in the laboratory work.

Finally, I also thank my family and my friend Bright Amponsah for his motivation and encouragement during the writing of the final thesis and throughout my studies at the university.

## ABSTRACT

The bio-based monomer, specifically acrylated methyl ester derived from sunflower oil, was incorporated to formulate polymer latexes for coating applications. The content of the bio-based monomer building units in the copolymer chain structure ranged from 5 to 30 wt. %. The emulsion polymerization of these bio-based monomers showed successful results, characterized by low coagulum levels (below 3%) and high monomer conversion rates (around 95%). The integration of the bio-based derivatives into the polymer latexes was confirmed by infrared spectroscopy. In addition, asymmetric flow fractionation coupled with multi-angle light scattering was used to analyze the molar mass distribution of the synthesized copolymers. The effectiveness of both anionic non-polymerizable and polymerizable emulsifiers was evaluated to determine the stability of the prepared latexes under elevated temperature conditions and their water resistance.

KEYWORDS

Emulsion polymerization, latex coating, bio-based monomer, polymerizable emulsifier, water resistance

CONTENTS

## LIST OF FIGURES

# LIST OF TABLES

## LIST OF ABBREVIATIONS

ADH: Adipic acid dihydrazide,

AF4- MALS: asymmetric flow field flow fractionation coupled with a multi- angle light scattering,

AME_SO: acrylated methyl esters of sunflower oil,

AMP 95: 2-amino-2-methyl-1-propanol,

BA: butyl acrylate,

BPO: benzoyl peroxide,

CMC: critical micelle concentration,

DAAM: diacetone acrylamide,

DLS): dynamic light scattering,

DMP: differential microemulsion polymerization,

MAA: methacrylic acid,

MEK: methyl ethyl ketone,

MFFT: minimum film forming temperature,

OWRK: Owens-Wendt-Rable-Kaelble,

RI: refractive index,

S: styrene,

$T_g$: Glass Transition Temperature,

THF: tetrahydrofuran,

# INTRODUCTION

In recent years, the quest for sustainable and environmentally friendly materials has become increasingly urgent due to concerns about climate change, resource depletion, and pollution. Within the realm of polymer science, the exploration of alternative monomers derived from renewable resources has gained significant attention as a promising avenue toward mitigating the environmental impact of traditional polymer synthesis processes [1,2]. Emulsion polymerization, a versatile technique widely employed in the production of various polymeric materials, offers a promising platform for the integration of bio-based monomers, thus enabling the development of eco-friendly polymers with diverse applications [3]. Emulsion polymerization involves the synthesis of polymers in the dispersed phase of an emulsion, typically consisting of water as the continuous phase and monomer droplets stabilized by surfactants or emulsifiers [4-7]. This process offers several advantages over conventional polymerization methods, including high reaction rates, control over particle size and morphology, and the ability to produce latex dispersions suitable for coatings, adhesives, and other applications [8,9]. By incorporating bio-based monomers derived from renewable sources such as vegetable oils [10], plant oils, sugars, or biomass, emulsion polymerization can further enhance its sustainability profile, reducing reliance on fossil fuels and minimizing carbon footprint [10-12].

This work aimed to utilize a bio-monomer in emulsion polymerization; specifically, acrylated methyl ester from sunflower oil, and evaluate its polymerizability in a standard composition based on styrene-butyl acrylate copolymer. In addition, the effect of a polymerizable emulsifier in the bio-monomer-based compositions was evaluated. The objectives were as follows: (i) to ascertain what percentage of the bio-monomer synthesized can be incorporated and yield favorable stability of the latexes synthesized and properties of final polymer coating materials; (ii) to compare the stabilizing ability of anionic non-polymerizable and polymerizable emulsifiers used in emulsion polymerization, (iii) of anionic non-polymerizable and polymerizable emulsifiers used in emulsion polymerization, (iii) to evaluate the above-mentioned effects on coating properties of resulting polymer materials.

# 1. THEORETICAL PART

## 1.1. Emulsion polymerization and its components

Emulsion polymerization is a versatile polymerization technique used to produce polymer dispersions or latexes. In this process, monomers are dispersed in an aqueous phase containing surfactants or emulsifiers to stabilize the monomer droplets [5]. The polymerization reaction takes place within these droplets, leading to the formation of polymer particles suspended in the continuous aqueous phase.

The main components of emulsion polymerization media involve monomer(s), dispersing medium, emulsifier, and free-radical initiator [13,14]. The dispersion medium is water in which hydrophobic monomers are emulsified by surface-active agents (surfactants or emulsifiers). When emulsifier concentration exceeds critical micelle concentration (CMC) it aggregates in the form of spherical micelles, so surface tension at the surface decreases, as a result, hydrophobic monomers enter the vicinity of micelle, and the reaction continues until all monomer droplets are exhausted and micelle containing monomers increase in size. Typical micelles have dimensions of 2–10 nm, with each micelle containing 50–150 emulsifier molecules [6]. Water-soluble initiators enter the micelle where free radical propagation starts. In general, monomer droplets are not effective in competing with micelles in capturing free radicals generated in the aqueous phase due to their relatively small surface area [15], so the micelle acts as a meeting site of water-soluble initiators and hydrophobic vinyl monomers. As polymerization continues inside the micelle, the micelle grows by monomer addition from monomer droplets outside and a latex polymer particle is formed. A schematic representation of emulsion polymerization is shown in **Figure 1**. Emulsion polymerization is carried out through three main intervals as shown in **Figure 2**.

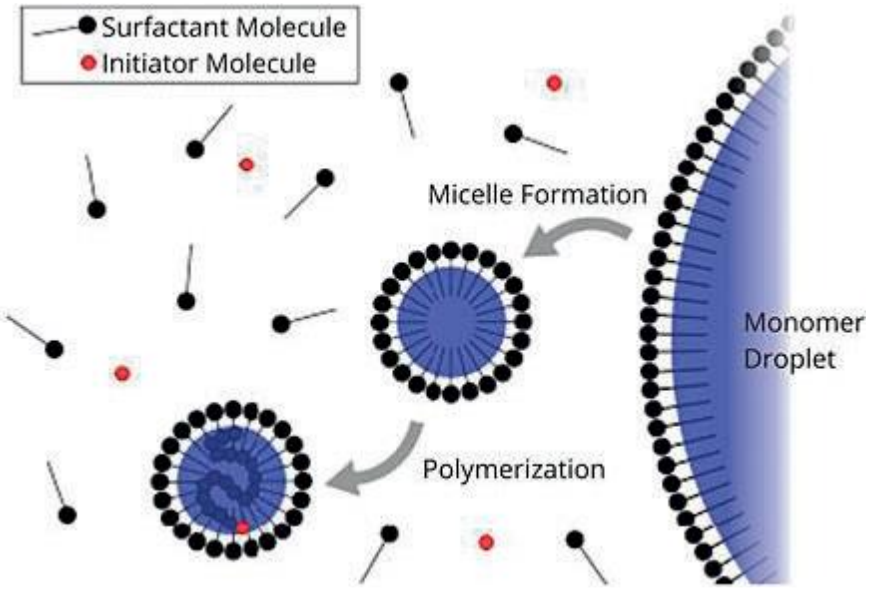


**Figure 1**. Schematic representation of emulsion polymerization [13].

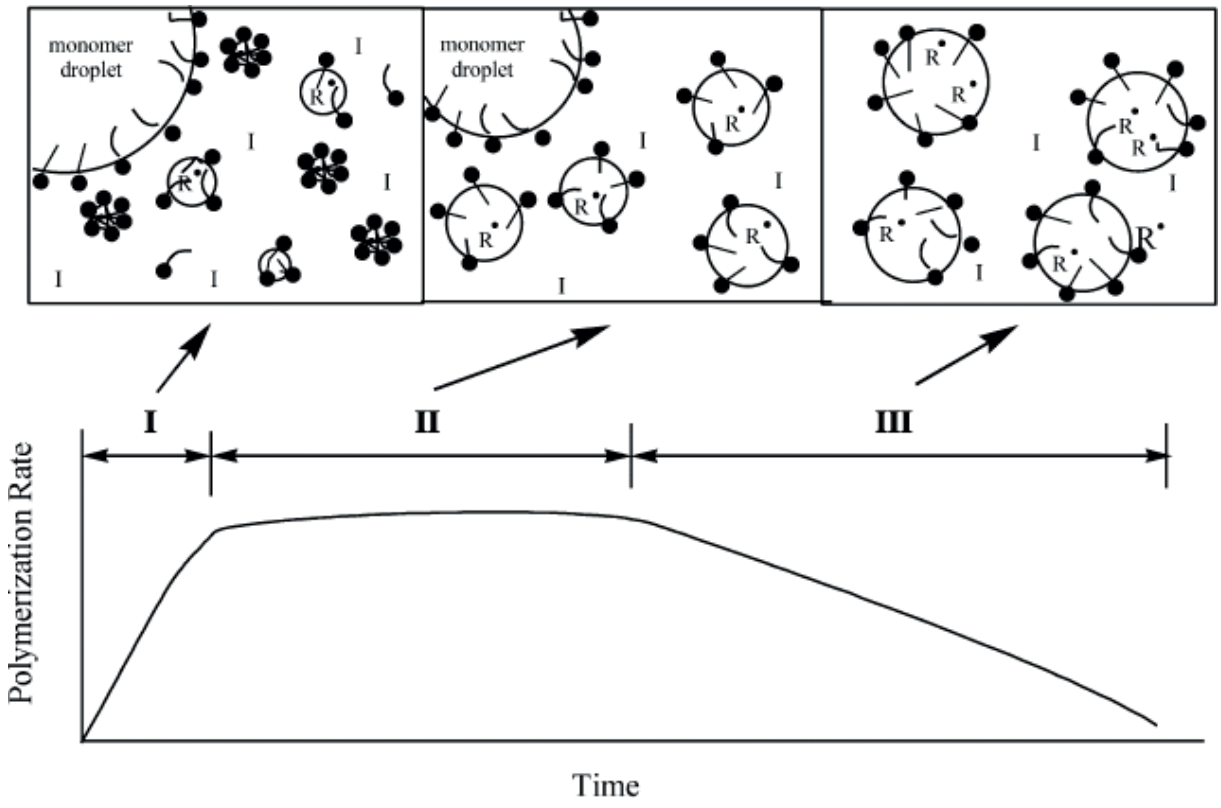


**Figure 2**. Emulsion polymerization intervals [13].

There is a separate monomer phase in interval I. The particle number increases with time in interval I and particle nucleation occurs in interval I. At the end of this stage, most emulsifiers are exhausted (i.e., micelles are exhausted) [15]. About one of every 102–103 micelles can be successfully converted into a latex polymer particle. The particle nucleation process is greatly affected by emulsifier concentration, which in turn affects particle size and particle size distribution of latex [6]. The lower the emulsifier concentration, the lower the nucleation period and the narrower the particle size distribution. At interval II (Particle growth stage), the polymerization continues, and polymer particles increase in size until monomer droplets are exhausted. Monomer droplets act as reservoirs to supply the growing particles with monomer and emulsifier species. At interval III, the polymer size increases as latex particles become monomer-starved and the concentration of monomer in the reaction loci continues to decrease toward the end of polymerization [6].

### 1.1.1. Initiators

Initiator acts to generate free radicals by thermal decomposition, or redox reactions. The initiators may be (i) water-soluble compounds like 2,2-azobis(2-amidinopropane) dihydrochloride, ammonium persulfate (APS), and hydrogen peroxide; (ii) partially water-soluble compounds like *t*-butyl hydroperoxide and succinic acid peroxide and azo compounds such as 4,4-azobis (4-cyanopentanoic acid) [16]; (iii) redox systems such as persulfate with ferrous ion, cumyl hydroperoxide or hydrogen peroxide with ferrous, sulfite, or bisulfite ion [17]; (iv) other initiators such as surface-active initiators, the so-called “inisurfs”, [18,19] for example, bis[2-(4′-sulfophenyl) alkyl]-2,2′ azodiisobutyrate ammonium salts and 2,2′-azobis(N-2′-methylpropanoyl-2-amino-alkyl-1-sulfonate). These initiators initiate emulsion polymerizat-ion without the need for stabilizers.

### 1.1.2. Emulsifiers

Emulsifiers, also called surfactants, act to decrease interfacial tension between the monomer and aqueous phase, stabilize the latex, and generate micelles in which monomers are emulsified and nucleation reaction proceeds [20]. Emulsifiers increase particle number and decrease particle size. Emulsifiers may be divided into several groups: (i) anionic emulsifiers such as fatty acid soaps (sodium or potassium stearate, laurate, palmitate), sulfates, and sulfonates (sodium lauryl sulfate and sodium dodecylbenzene sulfonate); (ii) nonionic emulsifier such as poly (ethylene oxide), poly

(vinyl alcohol) and hydroxyethyl cellulose; (iii) cationic emulsifiers such as dodecyl ammonium chloride and cetyltrimethylammonium bromide.

For ionic emulsifiers, micelles are formed only at temperatures above the Krafft point [16]. For nonionic emulsifiers, micelles are formed only at temperatures below the cloud point. Hence, emulsion polymerization is carried out below the cloud temperature and above the Krafft temperature [6].

Polymerizable emulsifiers (otherwise called reactive emulsifier or surfmers, usually comprising an active double bond) such as sodium dodecyl allyl sulfosuccinate [21,22] are also used to produce latexes with chemically bound surface-active groups [23,24]. Polymerizable emulsifiers consist of an amphipathic structure comprising a hydrophobic tail and hydrophilic head group [25], in addition to polymerized vinyl groups [26] in their molecular structure, which acquires them unique physicochemical properties other than traditional emulsifier moieties**.** They have surface activity like ordinary emulsifiers and reactive vinyl groups like vinyl monomers, so they can undergo polymerization reactions.

Due to their amphoteric structure and polymerization ability, polymerizable emulsifiers serve to synthesize inorganic/organic nanocomposites and are applied to emulsion polymerizations to stabilize formed latexes, or to prepare novel water-soluble hydrophobically associating polymers with strong thickening properties [27]. They are also greatly applied in the field of enhanced oil recovery [28]. Moreover, surfmers served as hydrophilic monomers to copolymerize with acrylamide derivatives forming hydrophobically associating polyacrylamide which acquired wide application in improved oil recovery coats and paintings, and drilling fluids [29]. Freedman et al. [30] reported the first synthesis of vinyl monomers which served as emulsifying agents [31]. Active vinyl groups were incorporated into allyls, acrylates, methacrylates, styryl and acrylamide [32]. Polymerized groups may be “H-type”, i.e., located in the hydrophilic head group, or “T-type”, i.e., located in the hydrophobic tail. They have a profound effect on emulsifier self-assembly and properties. Many kinds of polymerizable traditional emulsifiers, including cationic [33], anionic [34] and nonionic [35] have been synthesized to study the influence of the molecular structure, properties, and application of latex materials. Anionic polymerizable emulsifiers seem to be the most promising for utilization in coatings, adhesives, and enhanced oil recovery.

### 1.1.3. Dispersion medium

Water is the frequently used dispersion medium in emulsion polymerization as it is cheap and environmentally friendly. It represents the medium of transfer of monomers from droplets to particles and it is a solvent for emulsifiers, initiators, and other ingredients.

### 1.1.4. Monomers

Emulsion polymerizations require free radical polymerizable monomers. Generally, vinyl monomers are used in this type of polymerization such as acrylamide, acrylic acid, butadiene, styrene, acrylonitrile, acrylate ester and methacrylate ester monomers, vinyl acetate, vinyl chloride [16] and many other vinyl derivatives [20]. Depending on monomer solubility in the aqueous phase, there are three categories of typical emulsion polymerization monomers which comprise (i) monomers of high solubility, such as acrylonitrile; (ii) monomers of medium solubility, such as methyl methacrylate; (iii) monomers insoluble in the aqueous phase, such as butadiene and styrene [36].

### 1.1.5. Other constituents

Other components usually involve the emulsion polymerization medium that is generally deionized water. Antifreeze additives, such as inorganic electrolytes, ethylene glycol, glycerol, methanol, and monoalkyl ethers of ethylene glycol, allow polymerization at temperatures below 0 °C. Sequestering agents are used to solubilize the initiator system or to deactivate traces of hardness elements ($Ca^{+2}$, $Mg^{+2}$ ions) such as ethylene diamine tetraacetic acid or its alkali metal salts. Buffers, such as phosphate or citrate salts, are used to stabilize the latex toward pH changes [17]. Chain transfer agents, typically mercaptans, are frequently utilized.

## 1.2. Emulsion polymerization mechanism

Emulsion polymerization obeys a free radical polymerization protocol that occurs in three distinct steps, namely initiation, propagation, and termination.

### 1.2.1. Initiation

The initiation involves the decomposition of the initiator to free radicals either by hemolytic fission (hemolysis) through thermal decomposition or radiation and by chemical reaction through redox reactions.

The rate of initiator dissociation ($R_d$) is the rate-determining step and is given by Eq. (1). The rate of initiation ($R_i$) is given by Eq. (2).

$$R_d = 2f \cdot k_d \cdot [I] \quad (1)$$

$$R_i = 2fk_i [I] \quad (2)$$

where $k_d$ is the rate constant of initiator dissociation, $f$ is the initiator efficiency, [I] is the initiator concentration, and $k_i$ is the rate constant of initiation.

### 1.2.2. Propagation

The propagation involves the continuous addition of the monomer to active centers to form a polymer chain.

The rate of polymerization ($R_p$) is given by Eq. (3).

$$R_p = ki [R\bullet] [M] + k_p [M\bullet] [M] \quad (3)$$

Where [R•] is the free radicals' concentration, [M] is the monomer concentration, [M•] is the total concentration of active monomers, and $k_p$ is the rate constant of propagation. Since the amount of consumed monomers in the initiation stage is very small as compared to propagation, the term " $k_i$ [R•] [M] " can be neglected and the rate of polymerization is determined by the rate of propagation which is given by Eq. (4).

$$R_p = k_p [M\bullet] [M] \quad (4)$$

### 1.2.3. Termination

The termination leads to the loss of two growing polymer chains [37]. It occurs by either recombination or disproportionation. Recombination involves the reaction of one polymer chain with another growing one and reactive sites are blocked. Disproportionation is the case where one chain abstracts a hydrogen proton from another leaving it with an unsaturated end group. This termination mechanism results in two polymer chain fractions, where one is saturated, and the other is unsaturated [38].

Termination may also occur by chain transfer reactions. They involve the transfer of an active free-radical center from a growing polymer chain to another molecule or another site on the same polymer chain. In the case of transferring the active site to another molecule (called chain transfer agent), the polymerization reaction may further proceed, or the activated molecule cannot take part in the polymerization reaction at all, therefore, the propagation progress ceases [38].Literature on

the termination deals with the addition of retarders or inhibitors like phenols and catechols being frequently used to terminate active sites [39].

### 1.2.4. Kinetics of emulsion polymerization

The rate of polymerization is expressed by Eq. (5)

$$R\mathrm{p} = k_\mathrm{p}\,[\mathrm{M}\bullet]\,[\mathrm{M}] \tag{5}$$

Where [$M$•] is expressed by Eq. (6)

$$[\mathrm{M}\bullet] = N\,N_\mathrm{A}\,n \tag{6}$$

Where $N$ is the concentration of micelles, $n$ is the average number of radicals per micelle, $N_\mathrm{A}$ is the Avogadro number.

The rate of polymerization can also be expressed by Eq. (7).

$$Rp = N\,\mathrm{n}\,kp\,[M]\,N_A \tag{7}$$

The value of "n" determines the rate of polymerization and depends on radical diffusion out of the polymer particles (desorption), the particle size, modes of termination, and the rates of initiation and termination relative to each other and to the other reaction parameters [6].

Depending on the "n" value there are three cases that can be summarized: (i) emulsion polymerization mechanism for n = 0.5, where at any given moment half of the polymer particles contain one radical and are growing while the other half are dormant and known as zero–one system to indicate that a polymer particle contains either zero or one radical at any given moment [6]; (ii) emulsion polymerization mechanism for n < 0.5, where radical desorption from particles and termination in the aqueous phase are low, especially for small particle sizes and low initiation rates, (iii) emulsion polymerization mechanism for n > 0.5, where particle size is large, or the termination rate constant is low while termination in the aqueous phase and the initiation rate are fast, as some polymer particles contain two or more radicals.

The degree of polymerization ($X_\mathrm{n}$) is defined as the rate of growth of a polymer chain divided by the rate at which primary radicals enter the polymer particle and given by Eq. (8).

$$X_n = Nk_p\,[M]\,R\,I \tag{8}$$

The number of polymer particles is dependent on the total surface area occupied by emulsifier molecules in the system and is given by Eq. (9).

$$N = K\,(R\mu\,i\,)^{2/5}(a_\mathrm{s}\,\mathrm{S})^{\,3/5} \tag{9}$$

Where $a_s$ is the interfacial surface area occupied by a surfactant molecule, S is the total concentration of emulsifier in the system (micelles, solution, monomer droplets), μ is the rate of volume increase of polymer particle. The number of polymer particles can be increased by increasing the emulsifier concentration while maintaining a constant rate of radical generation.

### 1.2.5. Nucleation of particles

In general, nucleation is the first step in which monomers, e.g., atoms, ions, or molecules, form a new thermodynamic configuration or structure at the atomic or molecular level, followed by growth during which monomers are incorporated onto the surface of the nuclei, which may also coalesce or aggregate, leading to an increase in size [40]. Nucleation is a fundamental process in physical chemistry and materials science that involves the formation of new phases or particles from a supersaturated or undersaturated solution or vapor. It is a crucial step in various natural and industrial processes, ranging from the formation of raindrops in the atmosphere to the synthesis of nanoparticles in chemical reactions [41,42].

For a typical semi-batch emulsion polymerization system, the initial reactor charge comprises water, emulsifiers, and sometimes a small proportion of monomers. When the reaction temperature (e.g., 80 ° C) is reached, a persulfate initiator solution is added to the initial reactor charge to generate free radicals. This is then followed by the continuous addition of monomers (or monomer emulsion) over a period (normally a few hours). The appearance of the reaction mixture is transformed from transparent into translucent, opaque, and then milky white with the progress of polymerization, which reflects the nucleation and growth of latex particles [43].

#### 1.2.5.1. Homogeneous nucleation mechanism

Homogeneous nucleation occurs in a homogeneous system, where the nucleation event arises from fluctuations in the entire system [44]. It requires high levels of supersaturation or supercooling and typically leads to the formation of small nuclei with uniform size and shape. Waterborne initiator radicals are generated by the thermal decomposition of the initiator, and they can grow via the propagation reaction with monomer molecules dissolved in the aqueous phase. The oligomeric radicals then become water-insoluble when a critical chain length is reached. The hydrophobic oligomeric radical may thus coil up and form a particle nucleus in the aqueous phase. This is followed by the formation of stable primary particles via the limited flocculation of the relatively unstable particle nuclei and the adsorption of emulsifier molecules on their particle surfaces. The

emulsifier species required to stabilize these primary particles come from those dissolved in the aqueous phase and those adsorbed on the monomer droplet surfaces [5].

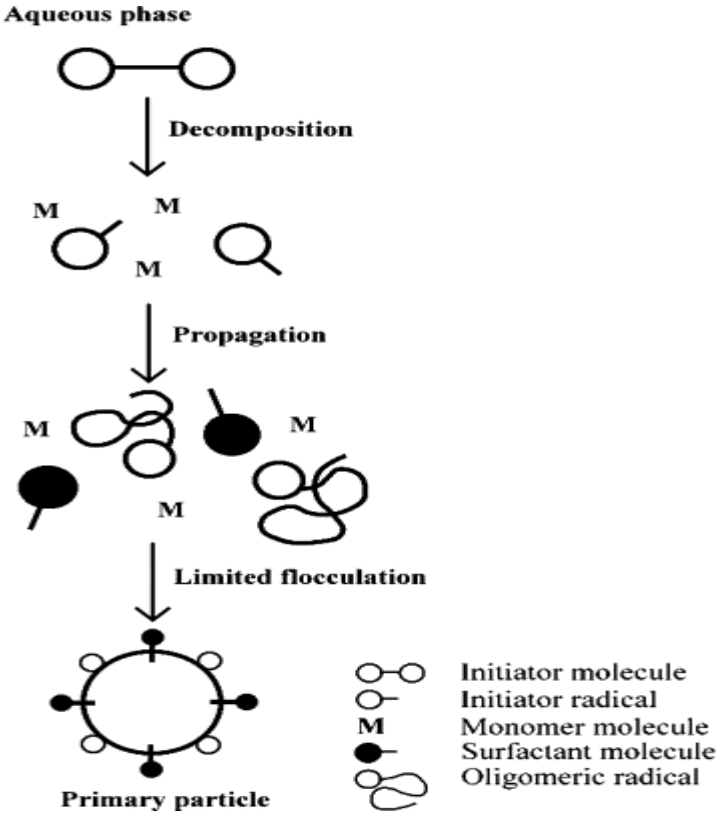


**Figure 3**. A schematic representation of the homogeneous nucleation mechanism [5].

## 1.2.5.2. Micellar nucleation

Based on the micellar nucleation mechanism, monomer initiation, and polymer chain growth occur within a micelle. The common features of these two phenomena are that the polymer nanoparticle precursors exist within the micelles and require an emulsifier to stabilize, as shown in **Figure 4**. If the concentration of the emulsifier is sufficient to provide enough micelles to encapsulate all the generated and newly formed precursors, the particle size will be stable and minimized. The threshold concentration of the emulsifier at this point is, therefore, the Critical micelle concentration (CSC) [46].

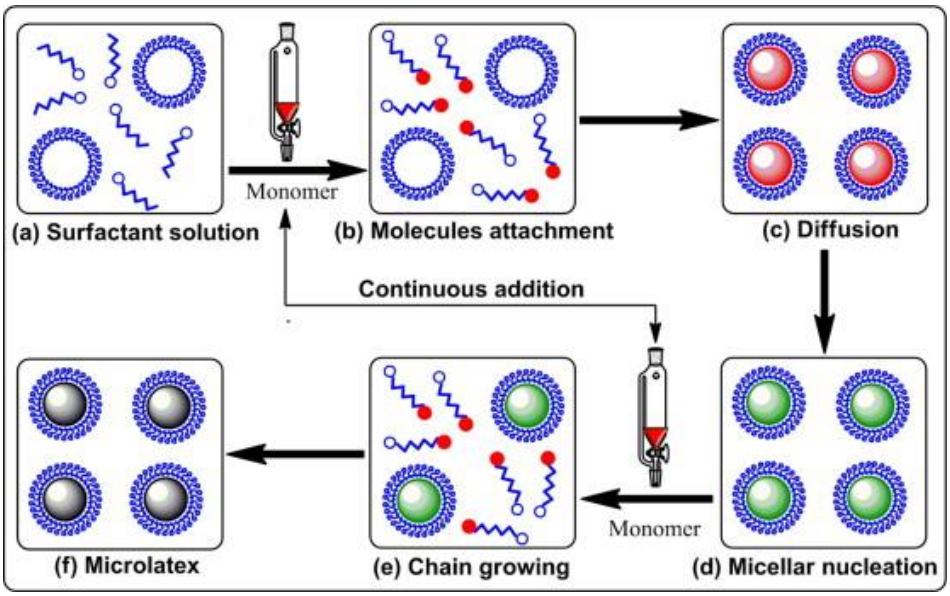


**Figure 4**. Schematic illustration of the functional mechanism of the benzoyl peroxide (BPO) initiation differential microemulsion polymerization (DMP) system. The blue color stands for emulsifier molecules. Red color stands for the monomer molecules. The green color stands for growing polymer chains. The black color stands for polymer nanoparticles [46].

## 1.3. Film formation and minimum film forming temperature

When a latex dispersion is applied to a substrate and allowed to evaporate, a continuous, homogeneous film will form under appropriate conditions. This process is known as film formation [47]. Ironically, much effort is put into keeping the particles separate and deflocculating in latex synthesis to obtain a stable dispersion. However, these same particles must overcome their mutual repulsion during film formation to form a continuous film. Not surprisingly, emulsifiers and stabilizers are often found to inhibit film formation.

The term "film formation" is used in more than one way in literature and, therefore, has more than one meaning. Sometimes, the term describes the whole process by which an aqueous polymer dispersion is converted into a continuous coating [48]. Some researchers refer to the various "stages of film formation" and thus invoke this meaning of the term. Although the names of the stages vary between authors, there are three primary physical processes or stages that occur during film formation: (i) evaporation of water and particle ordering, (ii) particle deformation, and (iii) interdiffusion of polymers across particle-particle boundaries. Dillon [48] first proposed in 1953

that film formation consisted of evaporation and particle deformation [49]. Later, Voyutskii [50] commented that "autohesion" (or diffusion leading to the dissolution of internal boundaries) follows the previous two stages. Following a different convention, other authors have used "stage" to describe morphologies linked by sequential physical processes. In this usage, latex evolves from one stage to another: from a colloidal dispersion to a dense packing of particles, to a densely packed array of deformed particles, and finally, to a continuous material. Some researchers refer to the "onset of film formation" as the point of optical clarity or mechanical integrity in a drying latex coating.

The term of the mechanical integrity of a latex coating comes from the developers using the minimum film forming temperature (MFFT) test. Protzman and Brown [51] proposed the term MFFT and a method for determining it in 1960. A standard test, ASTM D-2354-68, directly derived from the work of Protzman and Brown, defines MFFT as the lowest possible temperature at which film formation occurs, as determined by visual observation of cracking or whitening [52]. An apparatus for measuring MFFT consists of a metal rod with a temperature gradient across it onto which latex is poured. The film becomes opaque at a certain point, corresponding to the MFFT. MFFT has also been measured using transmission spectrophotometry [53]. Eckersley et al. defined MFFT as "the minimum temperature at which a latex cast film becomes continuous and clear." Below this critical temperature, the dry latex is opaque and powdery" [54]. A similar definition was used by Winnik et al. [55]. between the "cracking point" (the temperature at which the latex becomes continuous and free of cracks) and the minimum temperature at which cloudiness disappears. They said that the point of optical clarity is usually at a lower temperature. While the crack point indicates the onset of particle-particle adhesion, the point of optical clarity indicates that the average pore size is well below the wavelengths of visible light. MFFT is the primary indicator of the lower temperature range over which latex can be used in coating applications. MFFT has been studied as a function of latex particle diameter [56], polymer shear modulus, time, polymer surface tension, copolymer composition [57], latex polymer glass transition temperature [58], plasticizer content, polymer hydrophobicity, relative humidity, shell thickness of a core-shell latex [58] freeze-thaw stability [59], pH, and emulsifier type and concentration.

## 1.4. Emulsion polymerization of bio-based monomers

Bio-based monomers are organic compounds derived from renewable biomass sources, such as plants, algae, or waste materials, that serve as the building blocks for polymer synthesis [60,61]. These monomers offer environmental benefits over traditional petroleum-based monomers by reducing dependence on fossil fuels and mitigating greenhouse gas emissions[9], [62-64]. Bio-based monomers can be classified based on their chemical structure, origin, or application as follows: (i) Sugar-derived monomers obtained from sugars, such as glucose, fructose, xylose, and levulinic acid. (ii) Vegetable oil-based monomers derived from vegetable oils like soybean oil [65], castor oil [1,66], and palm oil. These compounds may have the chemical structure of fatty acids, and fatty acid esters (FAMEs) [67]. (iii) Cellulosic and lignin-derived monomers obtained from cellulosic or lignin-rich biomass sources. Examples include cellulose acetate and lignin-based phenolic monomers. (iv) Biogas and waste monomers produced from organic waste streams or biogas fermentation. Examples include lactic acid, succinic acid, and methane.

Other bio-based monomers in emulsion polymerization also include: (i) Acrylic acid that can be derived from bio-based sources such as sugar or glycerol. It is used to produce polymers such as polyacrylic acid and its derivatives which are used in adhesives, coatings, and superabsorbent polymers [68-71]. (ii) Vinyl acetate that can be produced from bio-based ethanol derived from renewable resources. It is a key monomer in the production of vinyl acetate-ethylene copolymers used in coatings, adhesives, and textile applications [72]. (iii) Lactic acid which is derived from renewable resources such as corn starch or sugar cane. It can be polymerized to produce polylactic acid, a biodegradable polymer used in packaging, textiles, and biomedical applications [73-75]. (iv) Styrene that can be produced from bio-based feedstocks such as lignocellulosic biomass or waste streams. Bio-based styrene is used in the production of styrene-butadiene latex polymers for coatings, adhesives, and carpet backing. (v) Methacrylic acid [68] can be synthesized from bio-based feedstocks such as glycerol or bio-based propylene [76]. It is used to make poly (methyl methacrylate) [77] and its copolymers for automotive, construction, and electronics applications.

# 2. EXPERIMENTAL PART

## 2.1. Chemicals

Latexes were prepared of commercial monomers, specifically butyl acrylate (BA, CAS: 141-32-2), methacrylic acid (MAA, CAS: 79-41-4), styrene (S), and diacetone acrylamide (DAAM, CAS: 2873-97-4). All these monomers were purchased from Sigma-Aldrich (Prague, Czech Republic). Further, acrylated methyl esters of sunflower oil (AME_SO) were utilized in the synthesis of latexes. This compound was synthesized at the laboratories of the Department of Physical Chemistry and the Institute of Macromolecular Materials of the University of Pardubice.

Disponil FES 993 (BASF, Prague, Czech Republic) was used as an ordinary (non-polymerizable) anionic emulsifier. ADEKA REASOAP SR-10 (DKS Co.Ltd. (Tokyo, Japan). was used as the polymerizable anionic emulsifier. Ammonium persulfate (CAS: 7727-54-0, Penta, Prague, Czech Republic) was used as the initiator of the polymerization reaction. Adipic acid dihydrazide (ADH, CAS: 1071-93-8) was utilized as the covalent crosslinking agent and was purchased from TCI Europe (Zwijndrecht, Belgium)and 2-amino-2-methyl-1-propanol (AMP 95, Sigma-Aldrich, Schnelldorf, Germany, CAS: 124-68-5) as neutralizing agent. All these chemicals were utilized as received without any further treatment.

## 2.2. Synthesis of latexes

Two series of latexes were prepared using the technique of semi-continuous emulsion polymerization. The latex copolymers were composed of standard acrylic monomers (MMA, BA, DAAM, S) and bio-based monomer (AME_SO) of content (10, 20, and 30 wt. % in the monomer mixture). The latex samples were labeled as D_Y, and S_Y, where D and S represent (non-polymerizable) emulsifier and polymerizable emulsifier, respectively, and Y represents the percentage content of the bio-based monomer in the monomer mixture. The amounts of the emulsifiers were set to maintain the same content of surface-active matter in both types of latex samples. Concurrently, reference latex was synthesized from MMA, BA, DAAM, and S with their respective emulsifiers. The mass fraction of these monomers was maintained in all monomer compositions. The difference was the content of the bio-based monomer**.** The latexes were produced in a 700 mL glass reactor by semi-continuous two-stage emulsion polymerization under

starved conditions in a nitrogen atmosphere at 85 °C. This procedure ensured relatively homogeneous latex particles of statistical copolymers. The recipe for emulsion polymerization is shown in Table 1. The reactor charge was put into the reactor and heated to the polymerization temperature. Then, the monomer emulsion was fed into the stirred reactor within 60 min in two steps (1. first-stage polymer preparation, 2. second-stage polymer preparation). After that, the polymerization was completed during 2 h of hold period at 85 °C. The pH was adjusted to 8 with a 50% aqueous solution of AMP 95. To ensure the keto-hydrazide self-crosslinking of latexes, a 10 wt.% aqueous solution of ADH in the amount corresponding to the molar ratio ADH: DAAM = 1:2 was added to the latex under agitation (0.625 g ADH dissolved in 5.9 g water). Every latex composition was synthesized in duplicate.

**Table 1**. Composition of the reaction system

| Component | Chemicals used | Mass (g) |
|---|---|---|
| ***Reactor*** | | |
| Reaction medium | Demineralized water | 10.250 |
| Emulsifier | Disponil FES 993[a] | 0.125 |
| | SR-10[b] | 0.042 |
| Initiator | Aqueous solution of $(NH_4)_2S_2O_8$ (0.175 g $(NH_4)_2S_2O_8$ + 6 ml $H_2O$) | 6.175 |
| ***Monomer emulsion (first stage)*** | | |
| Reaction medium | Demineralized water | 23.000 |
| Emulsifier | Disponil FES 993[a] | 1.850 |
| | SR-10[b] | 0.617 |
| Monomers | S, BA, MAA, AME_SO | 25.000 |
| Initiator | Aqueous solution of $(NH_4)_2S_2O_8$ (0.175 g $(NH_4)_2S_2O_8$ + 6 ml $H_2O$) | 6.175 |
| ***Monomer emulsion (second stage)*** | | |
| Reaction medium | Demineralized water | 23.000 |
| Emulsifier | Disponil FES 993[a] | 1.850 |
| | SR-10[b] | 0.617 |
| Monomers | S, BA, MAA, DAAM, AME_SO | 25.000 |
| Initiator | Aqueous solution of $(NH_4)_2S_2O_8$ (0.175 g $(NH_4)_2S_2O_8$ + 6 ml $H_2O$) | 6.175 |

[a]Component used for D samples.
[b]Component used for S samples.

**Table 2**. Names of latex samples and the amount of respective monomers in the monomer mixture

| Sample | Bio-based monomer content (wt %) | Monomers (g) | | | | | | | | |
|---|---|---|---|---|---|---|---|---|---|---|
| | | First step | | | | Second step | | | | |
| | | S | BA | MAA | AME_SO | S | BA | MAA | DAAM | AME_SO |
| D_0 | 0 | 10.8 | 13.5 | 0.8 | - | 9.8 | 13.3 | 0.8 | 1.3 | - |
| D_10 | 10 | 9.7 | 12.1 | 0.8 | 2.5 | 8.7 | 11.8 | 0.8 | 1.3 | 2.5 |
| D_20 | 20 | 8.5 | 10.7 | 0.8 | 5.0 | 7.6 | 10.4 | 0.8 | 1.3 | 5.0 |
| D_30 | 30 | 7.4 | 9.3 | 0.8 | 7.5 | 6.6 | 8.9 | 0.8 | 1.3 | 7.5 |
| S_0 | 0 | 10.8 | 13.5 | 0.8 | - | 9.8 | 13.3 | 0.8 | 1.3 | - |
| S_10 | 10 | 9.7 | 12.1 | 0.8 | 2.5 | 8.7 | 11.8 | 0.8 | 1.3 | 2.5 |
| S_20 | 20 | 8.5 | 10.7 | 0.8 | 5.0 | 7.6 | 10.4 | 0.8 | 1.3 | 5.0 |
| S_30 | 30 | 7.4 | 9.3 | 0.8 | 7.5 | 6.6 | 8.9 | 0.8 | 1.3 | 7.5 |

## 2.3. Evaluation of latexes and coating films

The coagulum content, pH, solids content, and degree of conversion of the latexes were first determined. The asymmetric flow field flow fractionation coupled with a multi-angle light scattering detector was used to describe the molar mass distribution of the synthesized copolymers before alkalization and before the addition of ADH. Measurement of the viscosity of the resulting latex was also part of the basic tests, with the difference that the determination was performed not only before alkalization but also after alkalization with AMP 95 and the addition of ADH to latexes containing copolymerized DAAM.

After alkalization and addition of ADH, MFFT was measured. The stability of latexes was also evaluated, including the measurement of particle size, zeta potential, and determination of the resistance of the latexes to electrolytes, determination of storage stability (30 days at 40 °C), thermal stability (24, 48, and 120 h at 50 °C) as well as the mechanical stability of the latexes.

Coating films were created by applying latex material to glass substrates using an applicator with a uniform gap size of 120 µm. Coatings were made on four standard glass panels, one glass panel coated with matt black paint, and two glass slides. All the coatings were allowed to dry at room temperature 22±3 °C for 30 days. The coating films on glass panels were characterized in terms of

scratch hardness, which includes pencil and pendulum hardness, film thickness, appearance of the coating film, cross-cut test adhesion, pull-off test, and water whitening. The coating on the black plate was used for the tests to determine gloss and resistance to the action of methyl ethyl ketone (MEK). Glass slides were used to determine water contact angle. Cupping, impact resistance, and bending tests were evaluated for coating films on steel substrate.

To characterize the chemical structure of the synthesized copolymers and to determine the important properties of latex polymer films, such as the glass transition temperature ($T_g$), water absorption, the proportion of extractable water-soluble substances, the gel content, and the crosslink density, it was necessary to make free-standing films. To create the bodies, films from each latex were cast into a silicone mold (the wet film's thickness was approximately 1.2 mm). The resulting casts were left to dry for 30 days at laboratory temperature (22±3 °C) and then another two weeks in a vacuum oven at an elevated temperature (30 °C).

### 2.3.1. Determination of the content of the coagulum formed during the synthesis

By coagulum, we mean the amount of colloidal dispersion in mass units [g] formed during the polymerization reaction as a precipitate. The formation of this precipitate is usually conditioned by the poor stability of latex dispersion.

The coagulum was collected using a fine filter screen through which the latex material was passed after the completion of the polymerization reaction and cooling. This was followed by the determination of the amount of precipitated substance. The captured coagulum content was dried in an oven (50 °C) for 7 days and then weighed on an analytical balance. The actual content of the coagulum [%] was calculated according to Eq. (10) [78,79].

$$\text{coagulum content (\%)} = \frac{m_C}{\frac{m_2 \times m_L}{m_1} + m_C} \times 100 \quad (10)$$

where $m_1$ is the weight of a liquid latex portion, $m_2$ is the weight of the latex portion dried to a constant weight at 110 °C, $m_C$ is the weight of the dried coagulum, $m_L$ is the weight of the total filtered latex.

### 2.3.2. Determination of degree of polymerization conversion

The degree of conversion expresses the reaction transformations of monomer substances that lead to the formation of macromolecular chains. The greater the degree of conversion, the higher the degree of polymerization of the individual macromolecules, which results in a significant increase in the molecular weight of the polymer compared to its starting synthetic substances. In the emulsion technique, the total conversion is close to 100%, which means that almost all the monomers involved in the reaction processes react to a polymer substance.

During the actual determination of the degree of conversion, the procedure was carried out gravimetrically. A latex sample corresponding to a weight of 1±0.2 g was inhibited with 5% ethanolic solution of hydroquinone (2 drops), weighed onto a pre-weighed Petri dish. The sample was then dried for 120 min in an oven at 105 °C. The degree of conversion was again calculated as the arithmetic mean of three measurements according to Eq. (11) [78,79].

$$\text{monomer conversion (\%)} = \frac{\frac{m_2 \times m_T}{m_1} - (m_I + m_S)}{m_M} \times 100 \quad (11)$$

where $m_1$ is the weight of a liquid latex portion, $m_2$ is the weight of the latex portion dried to a constant weight at 110 °C, $m_T$ is the total weight of all the materials put in the reaction flask, $m_I$ is the weight of the initiator, $m_S$ is the weight of the emulsifier (active matter), $m_M$ is the weight of the total monomers.

### 2.3.3. Determination of pH value of latex

The ISO 1148 standard was used to determine the pH value of polymer dispersions. Before the actual measurement, it was first necessary to perform a calibration using buffers with a pH range of 4 and 7. A clean electrode rinsed with distilled water and properly dried was inserted into a beaker containing a sample with latex dispersion. After the potential had stabilized, the displayed value on the instrument display was recorded. After cleaning the electrode again and mixing the colloidal dispersion in the beaker, the measurement was repeated twice more for accuracy. In total, three measurements were therefore performed for each polymer dispersion and the resulting pH was calculated as the arithmetic mean of the three readings.

### 2.3.4. Determination of latex solid content

According to the standard ČSN EN ISO 3251 (67 3031), the amount of dry matter or the content of non-volatile components in each amount of latex dispersion is determined. The actual determination began by weighing a latex sample on an analytical balance in an amount of 1 g with an accuracy of ±0.2 g into a pre-weighed Petri dish lined with aluminum foil. Then, the dish containing the volatile and non-volatile components was placed in a drying oven for 60 min at a temperature of 105 °C. After 1 h, the dish was removed from the dryer and placed in the desiccator. After cooling to room temperature, the sample was weighed again on an analytical balance and the dry matter in [%] was calculated according to Eq. (12) [80].

$$Dry\ matter = \frac{Total\ dry\ mass}{Total\ wet\ mass} \cdot 100 \tag{12}$$

Measurements were performed to maintain accuracy for each sample a total of three times, and then the arithmetic mean was calculated to achieve the final value of latex dry matter.

### 2.3.5. AF4-MALS characterization latexes modified with bio-monomers

The molar mass distribution was determined using the asymmetric flow field flow fractionation coupled with a multi- angle light scattering (AF4- MALS). Styrene-butyl acrylate copolymers in the ratio of 54/43 with 3 % acrylic acid and various amounts of bio-monomer were used. Instrument for asymmetric flow field flow fractionation (AF4) was Eclipse from Wyatt Technology. Long channel with thickness 350 μm, membrane Ultracel PLCCC 5 kDa, mobile phase tetrahydrofuran (THF). Multi-angle light scattering (MALS) detector DAWN and refractive index (RI) detector Optilab, both from Wyatt Technology. Sample concentration ≈ 2,5 mg/mL v THF, injection 100 μl. MALS data evaluation: first peak of polymer: Zimm light scattering formalism; nanogel peak: 1st order Berry or 3rd order Debye formalism.

### 2.3.6. Determination of the apparent viscosity of latex according to Brookfield

This method was carried out according to the ČSN ISO 2555 standard, which is used for so-called non-Newtonian liquids, and the MPW351e centrifuge device (MPW Med. Instruments, Poland) was used as a measuring device. The viscosity of the test latex sample was measured at a constant rotation speed of the cylindrical spindle of 100 rpm. The spindle type was always selected so that the measurement showed torque values in the range of 10 to 90 %. The value of apparent viscosity

[cP = mPa·s] was read from the display after a period of 30s from the start of spindle rotation. Three measurements were again performed for each latex, where the final viscosity result for individual samples was subtracted from the arithmetic mean value.

### 2.3.7. Determination of the minimum film forming temperature (MFFT) of latex

MFFT is usually referred to as the temperature that is read from the device at the boundary between the part of the paint film containing cracks and the area of the film without visible cracks [81,82]. Determination based on the ISO 2115:1996 standard was carried out on the MFFT 60 device (RHH s.r.o., Czech Republic), which contains a metal plate forming the key essence of the entire measurement process. A temperature gradient is created using a metal plate, so the required temperature interval was set on the device from temperature T1 (–3 °C) to temperature T2 (13 °C) when the limit temperatures were set just at the edge of the plate. After tempering the device, a foil was placed on the plate, onto which the latex material was applied using a ruler to create an even coating film along its entire length. With the help of the heat generated by the device and the dry air supply, the coating film was subjected to gradual drying for about 3h. The drying time depends on the choice of program and the characteristics of the dispersion used. After the coating film had completely dried, MFFT was read using a temperature ruler at the already-mentioned interface. In total, determinations for the accuracy of the resulting measurement were made three times. The final numerical value of MFFT was then calculated again as the arithmetic mean of these results.

### 2.3.8. Storage stability of latex

The latexes were evaluated for stability in terms of storability at elevated temperatures. Samples of individual dispersions with a volume of 10 mL placed in glass bottles were placed for 1 month in a drying oven set at a temperature of 40 °C. Before and after exposure to elevated temperature, the size of the particles was measured using the dynamic light scattering method, and the zeta potential was determined.

### 2.3.9. Thermal and Freeze-thaw stability of latex

Three series of latexes with a volume of 10 mL placed in glass bottles were subjected to a temperature of 60 ℃ for 24, 48, and 120 h, respectively. After the time interval, the latex

dispersions were filtered through a fine sieve. Possible capture of the resulting coagulum was monitored on the meshes of the sieve, which is directly related to the poor stability of the emulsifier used.

Also, three series of latexes with a volume of 10 mL placed in glass bottles were subjected to temperatures of –5 °C, –10 °C, and –18 °C for 24 h, respectively. After the 24 h freezing period, the samples were allowed to thaw at ambient temperature for 48 h. This freeze-thaw cycle was performed 3 times for every tested freezing temperature in case the latex sample was able to recover after the freezing process. The freeze-thaw stability test was evaluated by observing whether there was no coagulation produced after the latex stability test.

### 2.3.10. Mechanical stability of latex

The mechanical stability of colloidal polymer dispersions was evaluated immediately after their synthesis. Latex samples of 10 mL volume were placed in 15 mL centrifuge tubes. The samples were then placed in the MPW 351e centrifuge device, (MPW Med. Instruments, Poland) which allowed up to four samples to be taken at the same time. Containers containing latex dispersions must not only be completely uniform in weight but also placed crosswise. Centrifuge allows, due to centrifugal force, to increase the strength of the gravitational field in containers containing samples and is thus able to separate substances of greater and lesser density. The measurement itself took place in a centrifuge for 15 min at 4500 rpm, and possible precipitation of particles in the sample was monitored. If no coagulum was present when the latexes were filtered through a fine sieve, sufficient mechanical stability of the given polymer dispersion was demonstrated.

### 2.3.9. Latex particle size determination by dynamic light scattering (DLS)

The DLS method was used to measure the size of the particles contained in the colloidal dispersion of the latex material, which makes it possible to determine the size of the particles in the submicron range. A key part of the process is a laser beam (see **Figure 5),** which, from the source, hits the system of mobile particles of the colloidal dispersion. Most of the light incident on the sample remains unscattered and passes through the sample unnoticed. However, part of the incident radiation is scattered by individual particles in the dispersion, which is then captured by the detector. The scattered rays interfere with each other and create either bright or dark areas on the detector. At the same time, the particles in the dispersion are constantly moving due to Brownian

motion, and it is true that the larger the particle, the slower it moves; conversely, the smaller it is, the faster it moves. This creates intensity fluctuations in the captured radiation (changes in dark and light areas). The speed of change in intensity is directly influenced by the speed of movement of the particle that scattered the given beam since the speed of change in intensity of the radiation falling on the detector correlates with the speed of movement of this particle. The device can then calculate the particle size from this correlation function [83]. The average particle sizes of the latex particles dispersed in the water phase were detected by dynamic light scattering (DLS) using a Litesizer 500 instrument (Anton Paar GmbH, Graz, -Austria) due to its performance, simplicity and versatility, which is among the most widespread systems in the field of measuring the properties of colloidal materials. The measurement was carried out at 25 °C.

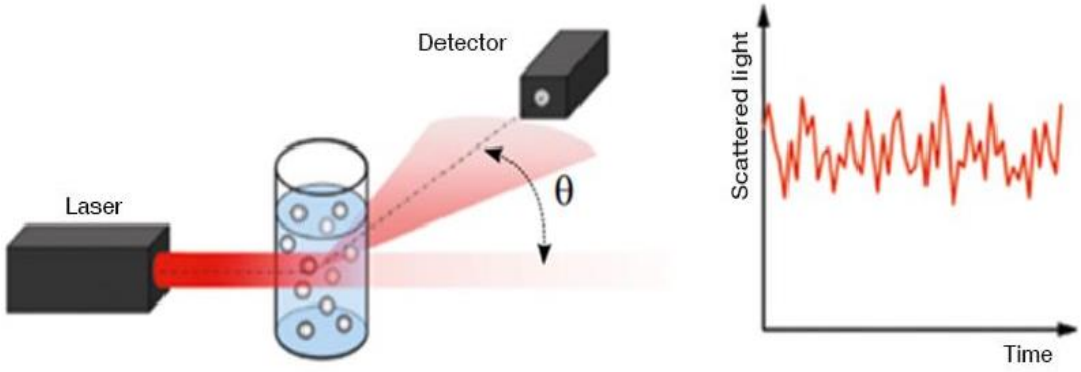


**Figure 5**. The working principle of DLS [83].

## 2.3.10. Determination of latex zeta potential by DLS

The principle of this method consists of creating an electrical double layer (see **Figure 6**) between the colloid particles and the dispersion medium. In other words, the formation of an electrically charged double layer takes part in charge of the colloidal particle, which is equivalently balanced by the number of oppositely charged ions of the polar solvent (water). Electrokinetic phenomena can then be imagined more closely as the interface between the so-called Stern layer, which is a

layer of counterions closely adjacent to the electrically charged particle, and the so-called diffusion layer, which are, on the other hand, ions far from the surface of the colloid particle.

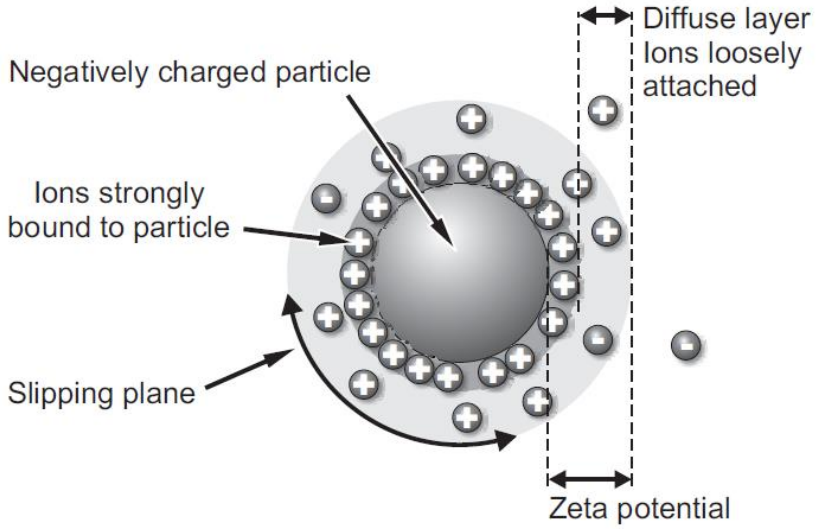


**Figure 6**. Representation of zeta potential [84].

The magnitude of the electrokinetic potential plays an important role in predicting the eventual stability of a colloidal polymer system and is directly related to its magnitude. If the system shows a large positive or negative zeta potential, then the particles are repelled from each other and their eventual precipitation to form a coagulum does not occur. Of course, in the opposite case, a small potential is not able to prevent their fluctuation and the particles become unstable. Furthermore, the zeta potential value is a function of pH. The determination of the zeta potential is therefore related to the emergence of electrokinetic phenomena, which can be carried out, for example, through electrophoresis. Applying an electric field to a system of particles in solution causes particles with closely packed opposite charges to move together toward one respective electrode, while distant ions are forced to move to the other oppositely charged electrode. Litesizer 500 instrument (Anton Paar GmbH, Graz, Austria), was used for the measurement. The measurements were carried out at 25 °C.

## 2.3.11. Determination of latex resistance to electrolytes

This test assessed the resistance of latexes to the influence of $CaCl_2$ electrolytes of different concentrations based on the absence or formation of precipitates in each latex sample. Calcium

chloride electrolyte was used. The actual determination was carried out in a concentration series from the highest values to those with the lowest electrolyte concentration. The following concentrations of electrolyte were used for testing: 0.01, 0.05, 0.1, 0.2, 0.5, 1, 1.5, 2, and 5 wt. %.

The measurement was carried out in several borosilicate tubes filled approximately half with the appropriate electrolyte solution of a certain concentration. The given latex sample was gradually introduced into the test tubes using a dropper (about two drops), and then the possible formation of a precipitate was observed. If a precipitate did not occur, the latex was considered resistant to a given concentration electrolyte.

### 2.3.12. Pendulum coating hardness test according to Persoz

A TQC SP0500 type pendulum device (Gamin, Czech Republic) corresponding to the ČSN EN ISO 1522 standard was used for this test. The principle of the pendulum test according to Persoz consists in measuring the number of swings of the instrument pendulum, which is placed using two steel balls (the diameter of one ball is 8 mm) on glass provided with a paint film. The pendulum is always lowered to the sample from the basic position, corresponding to a deflection (amplitude) of 12°, and the number of swings by which the amplitude is reduced to a value of 4° is recorded. The pendulum's return to the starting position is automatically ensured every time by means of a stepper motor, and the release of the pendulum is caused by an electromagnetic system. The pendulum, according to Persoz, is made of stainless steel and is suitable for soft surfaces, which include materials based on latex polymers. The number of swings is largely related to the hardness value of the paint film produced, and it is true that the higher the hardness of a particular material, the greater the number of swings.

Hardness measurement is one of the relative methods for which the presence of a reference substance (standard) is a necessary part, to which the measured value is always related. The resulting value [%] is therefore expressed in relative percentages according to Eq. (13) when a glass plate corresponding to the standard in the number of 430±15 swings was used as a reference substance.

$$\text{Relative hardness} = \frac{\text{Number of swings per latex coating}}{\text{Number of swings per glass standard}} \cdot 100 \quad (13)$$

Each sample was evaluated for the correctness of the resulting measurement three times, within 30 days. For each latex on individual days, the final film hardness value was calculated by averaging the measured values.

## 2.3.13. Determination of coating surface hardness

Determination of the surface hardness of latex coatings was carried out using the pencil method, which is governed by the rules according to the ČSN EN ISO 15184 standard. For our experiment, a set of pencils of the brand Hardthmuth KOHINOOR was used when the actual determination of the surface hardness of the material proceeded from pencils with the lowest hardness to pencils with higher hardness up to the pencil determining the final hardness of the latex coating within its tested surface. The resulting pencil determining the surface hardness of the material was the one that caused a permanent scratch on the coat film that could not be erased simply by using a finger. **Table 3** shows the types of individual pencils used to determine the hardness on the surface of the samples.

**Table 3**. List of used pencils

| **Number of pencils used** | 1 | 2 | 3 | 4 | 5 | 6 | 7 | 8 | 9 | 10 | 11 | 12 | 13 | 14 |
|---|---|---|---|---|---|---|---|---|---|---|---|---|---|---|
| **Pencil hardness** | 3B | 2B | B | HB | F | H | 3H | 4H | 5H | 6H | 7H | 8H | 9H | 3B |

## 2.3.14. Determination of coating thickness

The thickness of latex coatings was measured on glass plates according to the ČSN ISO 673061 standard. A three-point depth gauge was used to ensure the measurement itself, which evaluates the film thickness as a different value of the height of the central and edge point parts. To achieve the most accurate results, it was necessary to repeat the measurement at least three times for each sample and then determine the final value as an average of the measured instrument data. The thickness of the coatings on the steel panels was determined by an electromagnetic thickness gauge SAUTER TE 1250-0.1 FM (Sauter, Germany). The coating thickness was measured at three locations, from which the arithmetic mean was calculated.

## 2.3.15. Determination of coating adhesion by cross-cut test

The method governed by the ČSN ISO 2409 standard mainly determines the resistance of the coating film when it is cut through with a grid hand-held device. The cut on the coating was made in two mutually perpendicular directions, resulting in a grid with 2 mm distances between the individual cut lines. The test evaluation was performed visually according to the damage scale shown in **Table 4**.

**Table 4**. Evaluation of coating film adhesion

| Degree of adhesion | Description of the appearance of the created cross- cut |
|---|---|
| **0** | The edges of the cuts are smooth, no sign of a square peel mark |
| **1** | Slight peeling of the coating in the places where the grid cuts cross. The breach is not greater than 5% of the total grid surface. |
| **2** | Partial or complete peeling of coatings not only in intersecting sections but also along their longitudinal side. Surface damage in the range of 5–15% of the grid surface. |
| **3** | Partial or complete peeling of coatings not only in intersecting sections but also along their longitudinal side. Surface damage in the range of 5–35% of the grid surface. |
| **4** | Complete or partially peeled coating. Ranges damage in the 35–65% grid area. |
| **5** | Major damage to the paint film. |

## 2.3.16. Determination of coating adhesion by pull-off test

The test was performed on coatings with a wet film thickness of 120 µm applied on glass substrates using metal targets (diameter 20 mm) attached to the coating by means of two-component epoxy adhesive BISON Epoxy Universal. For measurement accuracy, 4 targets were placed on each coating film, and the values evaluated by the device were then arithmetically averaged. The measurement was carried out on an automatic pull-off meter Elcometer 510 (Gamin, Czech Republic) according to the ČSN EN ISO 4624 standard. The principle of the device is the measurement of the so-called minimum pull-off stress [MPa] at a specific speed of the pull-off force (0.2 MPa/s), which is necessary for the separation of the coating film from its substrate (in our case, glass).

## 2.3.17. Determination of the appearance of coatings

The appearance of the latex coatings on glass substrates was evaluated according to the criteria listed in **Table 5.**

**Table 5**. Visual properties of coating films on glass substrates

| Turbidity (T) | Bubbles (B) | Particles (P) | Surface (S) |
|---|---|---|---|
| T1 – no turbidity | B1 – without bubbles | P1 – none | S1 – smooth, fused surface |
| T2 – weak turbidity | B2 – isolated bubbles | P2 – 3 particles on an area of 1 $cm^2$ | S2 – brush marks |
| T3 – severe turbidity | B3 – bubbles throughout the area | P3 – 10 particles on an area of 1 $cm^2$ | S3 – dimples, craters, orange peel |
| T4 – whitening of the coating | | P4 – more particles | |

## 2.3.18. Determination of the gloss of coatings

Gloss measurement is a method that allows the revealing of the optical properties of a coat film in terms of its ability to reflect incident radiation. A Micro-TRI-9/gloss type gloss meter (BYK - Gardner, USA) was used to determine these optical properties, which are governed by the rules of the ISO 2813 standard. Coating films applied to the glossy side of the black-coated glass were subjected to the measurement of reflected light at angles of 20, 60, and 85 °. Since the gloss measurement is a relative method, the resulting gloss value had to always be considered against the reference material, represented by a shiny black plate with a refractive index of $n_D = 1.567$. The gloss meter always evaluated three gloss measurement results, with the evaluation quantity being the gloss number (GU) expressed as a percentage with respect to the standard for each coating angle, and then, via calculation, supplied the final value together with the relevant standard deviation.

## 2.3.19. Methyl ethyl ketone (MEK) coating resistance test

The principle of the method is the ability of the organic solvent 2-butanone (MEK) to dissolve the physical grouping of macromolecular chains or to swell the crosslinked structure of polymers. The

test was carried out according to the ASTM D 4752 standard using a glass rod on which wound a wad of cotton wool impregnated with the already-mentioned organic solvent. Strokes (approx. 5 cm) were made with a stick on the test coating at a constant frequency of movement speed (approx. 1 stroke/s). The result of the measurement was the time that corresponded to the breaking of the coating film.

## 2.3.20. Determination of the resistance of coatings in terms of water-whitening

After soaking in water, cotton wool was placed on top of the coating film cast on glass substrates, which was folded overusing Petri dishes to prevent its evaporation, and thus to ensure a constant effect of the liquid. The evaluation itself for individual latex coatings was carried out on a ColorQuest XE spectrometric device (Hunterlab, USA) in the place of the coating left in contact with water for 1, 4, and 24 h. The degree of whitening of the coating due to the action of water was evaluated by determining the transmittance at a wavelength of 500 nm. The degree of transparency of the material, or its whitening, was then determined by Eq. (14).

$$W = 100 \cdot (T_0 - T_t) / T_0 \tag{14}$$

where $W$ corresponds to the extent of whitening of the coating [%], $T_0$ represents the transmittance of the coating before the action of distilled water and $T_t$ represents the transmittance of the material after the experiment.

The greater the intensity of water-whitening after the action of water, the lower transmittance values were obtained, i.e., the less light passed through the coating sample. For the accuracy of the final determination of the whitening of coating films, all samples were evaluated a total of two times, when the subsequently calculated average value corresponded to the objective evaluation.

## 2.3.20. Tensiometric testing of coatings

Water and diiodomethane were used for tensiometric measurements in our experiment. An Attention Theta optical tensiometry device (Biolion Scientific, Finland) was used to measure the contact angle using the sitting drop method, and the One Attention software was available to process the acquired data. A 10 µl drop of the test solvent was applied to the glass slide using a micropipette. The average value of the contact angle was calculated from all three measurements, which were used to determine the material's surface energy. The surface energy [mN/m] of

individual coatings was calculated according to the Owens-Wendt-Rable-Kaelble (OWRK) method.

### 2.3.21. Determination of the glass transition temperature of emulsion copolymers

The glass transition temperature ($T_g$) plays an important role in characterizing all macromolecular substances. One of the thermal analysis methods generally used for the determination is differential scanning calorimetry (DSC). This method uses measured and comparative or reference samples to determine a specific quantity (see **Figure 7**). Both substances are subjected to linear heating or cooling in parallel and the power input, or the amount of energy supplied per time unit, must be supplied either to the sample (an endothermic process takes place in the sample) or to the reference substance (an exothermic process takes place in the sample) is usually measured so that the differences in temperature between them corresponded to a zero value. $T_g$ corresponds to the endothermic peak, as seen in **Figure 8**.

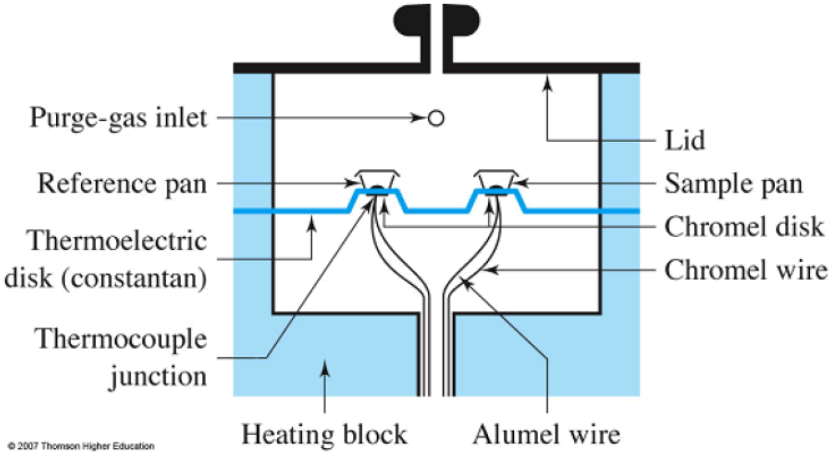


**Figure 7**. Equipment for DSC [85].

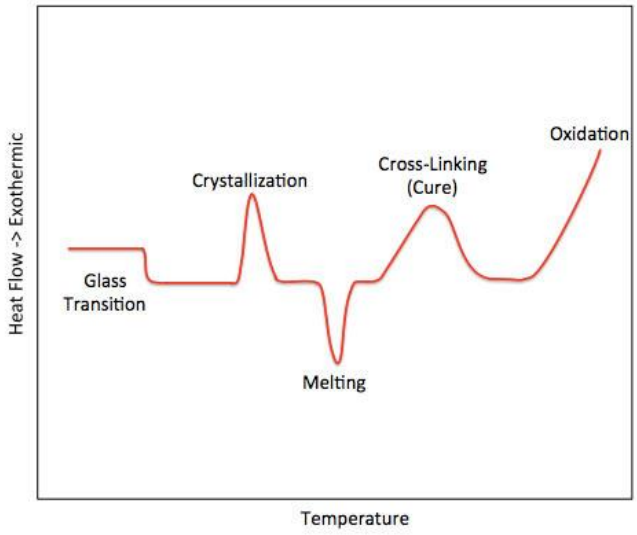


**Figure 8**. Illustration of the dependence of the heat flow value on the temperature [85].

## 2.3.22. Determination of water absorption

Three test samples with approximate dimensions of 2 × 2 × 0.1 cm were prepared from each free-standing film. The principle of the method was to determine the weight gain of individual specimens placed in distilled water after 1, 3, 7, 14, and 30 days. The coating film's water absorption [%] was calculated according to Eq. (15). The resulting value was determined as the arithmetic mean of the results of three bodies cast from each latex sample.

$$\text{Absorption} = \frac{m(wet\ sample - dry\ sample)}{m(dry\ sample)} \cdot 100 \quad (15)$$

## 2.3.23. Determination of gel content

The method is used to determine the degree of cross-linking of latex film by determining gel content. The more the macromolecular structure is cross-linked, the greater the percentage of the insoluble gel content in the relevant organic solvent. To determine the gel content, it was first necessary to dry the coating film sample and the cellulose cartridge for 48 h at 70 °C and immediately place them in a desiccator with pre-dried silica gel for 24 h. This was followed by weighing and recording the first value on the analytical balance. Then, the cartridge with the sample was placed in a Soxhlet extractor, where the 8-hour extraction of the sol of the latex sample began with the help of tetrahydrofuran solvent. After the end of the extraction, the sample with the cartridge was again placed in a drying oven at a temperature of 70 °C for 48 h. After 24 h of cooling

in a desiccator, reweighing followed. The gel content [%] that was not extracted by solvent was calculated according to Eq. (16).

$$\text{Gel content} = \frac{m(cartridge\ with\ sample\ after\ extraction - cartridge\ without\ sample)}{m(sample\ before\ extraction)} \cdot 100 \quad (16)$$

## 2.3.24. Determination of crosslink density

The method of determining the crosslink density is used to determine the actual degree of crosslinking of the macromolecules of the polymer dispersion. The basis of this test was the gravimetric measurement of the swelling of the respective network of the sample in toluene, in which it was placed in a drying oven at a temperature of 50 °C for one week. As part of this method, samples with an approximate weight of 0.2 g were used, extracted in a Soxhlet extractor according to the ČSN EN ISO 6427 standard, and the increase in their weight was subsequently measured after the exposure time of the body in the solvent. The following formulas Eqs. (17-20) were used to calculate the crosslink density [mol nodes/cm$^3$], which are based on the Flory and Rehner theory.

$$Crosslink\ density = \frac{\rho_p}{M_c} \quad (17)$$

where $\rho_p$ is the polymer density [g/cm$^3$], and $M_c$ is the average molecular weight of the polymer chain between two network nodes [g/mol].

The average molecular weight of the polymer chain between two nodes of the network was calculated according to Eq (18):

$$M_c = \frac{V_1 \rho_p [\phi^{\frac{1}{3}} - \frac{\phi}{2}]}{-[\ln(1-\phi) + \phi + \chi\phi^2]} \quad (18)$$

where $V_1$ is the molar volume of toluene [cm$^3$/mol], $\rho_p$ is the density of the polymer [g/cm$^3$], $\phi$ is the volume fraction of the swollen gel polymer and $\chi$ is the interaction parameter between toluene and the polymer.

The volume fraction of the swollen gel polymer was calculated according to Eq (19):

$$\phi = \frac{m_p \rho_s}{m_p \rho_s + m_s \rho_p} \quad (19)$$

where $m_p$ is the mass of the polymer gel [g], $m_s$ is the mass of the solvent [g] and $\rho_s$ is the density of toluene [g/cm$^3$] and $\rho_p$ is the density of the polymer [g/cm$^3$].

The interaction parameter was calculated according to Eq (20):

$$\chi = 0{,}34 + \frac{V_1}{RT}(\delta_p - \delta_s) \quad (20)$$

where $V_1$ is the molar volume of toluene [$cm^3$/mol], R is the universal gas constant [$JK^{-1}mol^{-1}$], T is the laboratory temperature [K], $\delta_p$ is the copolymer solubility parameter [$(cal/cm^3)^{1/2}$], $\delta s$ is the solvent solubility parameter [$(cal/cm^3)^{1/2}$].

## 2.3.25. Determination of incorporation of bio-based monomers into latex copolymers

Fourier transform infrared (FT-IR) spectroscopy was used to detect the incorporation of vegetable oil-based monomers into latex copolymers. Infrared spectra of the samples were recorded on a Nicolet iS50 FTIR spectrometer (Thermo Fisher Scientific, Waltham, MA, USA) using a built–in diamond ATR (attenuated total reflection) crystal in the region of 4000–400 $cm^{-1}$ (data spacing = 0.5 $cm^{-1}$).

## 2.3.26. Cupping test

The cupping test was evaluated in accordance with the CSN EN ISO 1520 standard. The TESTER 102004007 deepening device (Elcometer Great Britain) was used as a measuring device.

## 2.3.27. Falling weight test

The falling weight test was evaluated in accordance with the CSN EN ISO 6272 standard. Elcometer, Germany) was used as the measuring device.

# 3. RESULTS AND DISCUSSION

## 3.1. Evaluation of properties of latexes

Two series of polymer dispersions were prepared and differed in the type of emulsifier used. The first series was made from a non-polymerizable emulsifier (Disponil FES 993, labeled D-series), and the second series with a polymerizable emulsifier (SR-10, labeled S-series). In each of the series, individual samples of aqueous polymer dispersions differed in the included bio-based monomer AME_SO content.

From **Table 6,** the hydrodynamic diameter of the latex dispersions increased in the final stage of the synthesis, which may indicate no further particle nucleation but only particle size growth. This phenomenon also indicates that a second-stage polymer rich in copolymerized DAAM building units was formed in the outer layer of latex particles, which is beneficial for subsequent inter-particle keto-hydrazide crosslinking. Regarding the polydispersity (PDI), the values imply unimodal and narrow particle size distribution for all the prepared latex samples. In most cases, the zeta potential decreased slightly in the final stage except for D_0 and S_30.

From **Table 7,** the pH value of the polymer dispersions increased in the dispersions with 30 wt. % content of bio-based monomer. D_0 without bio-based monomer had a pH value of 2.0±1.1, and D_30 with 30 wt. % content of bio-based monomer had a pH of 4.2±1.5. In addition, the same trend occurred in the S series with S_0 of pH 1.9±0.5 and S_30 with pH 5.0±0. It was noticed that the type of emulsifier did not pronouncedly affect the pH of latexes, notwithstanding the bio-based monomer affected the pH of the latexes.

The experimentally determined dry matter content ranging from 35.9–39.7 wt. % correlated with the calculated theoretical value of dry matter, which is approximately 40 wt. %. The degree of conversion reached almost 100 % for the polymerizable emulsifier series without any bio-based monomer content incorporated (S_0) and 92.2 % when 30 wt. % of the bio-based monomer was incorporated. It can be stated that the polymerizable emulsifier had a relatively better effect on conversion compared to the non-polymerizable emulsifier. Nevertheless, a high ratio of monomers reacted to form a polymer chain in both series. It can, therefore, be concluded that the polymerizable emulsifier used positively affected the course of emulsion polymerization.

**Table 6**. Results of particle size, polydispersity (PDI), and zeta potential of latex samples of the first synthesis step and after finishing the polymerization process

| Sample name | After the first synthesis step | | | End of polymerization | | |
|---|---|---|---|---|---|---|
| | Hydrodynamic diameter (nm) | PDI (%) | Zeta potential (mV) | Hydrodynamic diameter (nm) | PDI % | Zeta potential (mV) |
| D_0 | 104.5±1.4 | 3.8±1.9 | -34.9±1.0 | 134.5±0.9 | 4.3±3.9 | -38.5±1.9 |
| D_10 | 80.5±0.9 | 7.4±1.1 | -60.8±5.7 | 124.1±2.4 | 2.8±1.5 | -54.0±1.1 |
| D_20 | 100.5±5.7 | 5.3±1.4 | -51.2±9.1 | 137.8±1.8 | 4.6±1.7 | -47.2±1.0 |
| D_30 | 70.4±1.3 | 3.9±4.2 | -63.1±3.1 | 94.0±1.6 | 4.2±3.1 | -57.5±12.7 |
| S_0 | 95.0±0.6 | 5.8±0.4 | -41.0±2.2 | 139.4±1.2 | 2.9±1.7 | -39.4±0.5 |
| S_10 | 98.0±1.5 | 6.4±2.9 | -57.8±12.8 | 141.8±2.2 | 6.4±4.4 | -45.2±1.1 |
| S_20 | 87.3±1.0 | 7.6±3.0 | -60.1±5.8 | 120.5±1.2 | 5.0±2.8 | -49.4±0.8 |
| S_30 | 79.0±1.3 | 5.6±3.4 | -55.7±7.0 | 107.8±1.3 | 7.1±2.0 | -57.7±10.8 |

**Table 7.** Overview of latex characteristics regarding pH, solid content, and conversion. The latexes were evaluated before the alkalization and ADH addition

| Sample name | pH (before alkalization) | Solids content (wt.%) | Conversion (%) |
|---|---|---|---|
| D_0 | 2.0±1.1 | 37.6 | 93.5 |
| D_10 | 2.1±0.8 | 37.0 | 98.0 |
| D_20 | 2.0±0.4 | 38.4 | 89.8 |
| D_30 | 4.2±1.5 | 35.9 | 89.4 |
| S_0 | 1.9±0.5 | 38.1 | 99.9 |
| S_10 | 2.0±1.2 | 39.7 | 98.8 |
| S_20 | 1.9±1.4 | 39.3 | 98.3 |
| S_30 | 5.0±0.1 | 37.1 | 92.2 |

Regarding the viscosity (see **Table 8**), the measured data reveal that adding AMP 95 and ADH did not significantly affect the viscosity of the polymer dispersions in both series. Viscosity values remained practically unchanged even after the alkalization of the latexes, so there was no unwanted swelling of polymer particles due to alkalization or destabilization of the polymer system. An

unusual increase in the S_10 sample from 16.1±0.5 to 26.4±0.6 might have contributed to measurement error.

**Table 8.** The viscosity of latex samples before and after adding AMP 95 and ADH

| Sample name | Initial viscosity (mPa·s) | Final viscosity (mPa·s) |
|---|---|---|
| D_0 | 14.9±1.0 | 13.7±1.3 |
| D_10 | 15.5±2.7 | 14.6±0.0 |
| D_20 | 16.6±2.9 | 16.6±0.2 |
| D_30 | 14.1±1.3 | 14.5±0.1 |
| S_0 | 14.7±1.5 | 13.5±1.2 |
| S_10 | 16.1±0.5 | 26.4±0.6 |
| S_20 | 20.5±0.8 | 21.8±1.1 |
| S_30 | 16.1±0.1 | 15.6±0.5 |

## 3.2. Stability of latexes

**Table 9** presents the data of the measured average particle size, PDI, and the zeta potential of aqueous polymer dispersions after synthesis when AMP and ADH have been added and subsequent storage for 1 month at a temperature of 40 °C. The values of particle size polydispersity and zeta potential did not change pronouncedly, which indicates the long-term storage stability of the synthesized polymer dispersions. It was noticed that the emulsifier type and the bio-based monomer content did not affect latexes' storage stability. In the D series, it was observed that the higher the particle size, the smaller the value of the zeta potential of the respective sample.

**Table 9**. Comparison of characteristics of final latex formulations before and after one month of storage at 40 °C

| Sample name | After synthesis | | | After one month of storage | | |
|---|---|---|---|---|---|---|
| | Hydrodynamic diameter (nm) | PDI % | Zeta potential (mV) | Hydrodynamic diameter (nm) | PDI % | Zeta potential (mV) |
| D_0 | 115.5±2.3 | 3.5±2.2 | -46.2±0.7 | 137.9±3.1 | 5.0±1.2 | -38.7±0.5 |
| D_10 | 124.0±3.7 | 2.5±1.6 | -40.4±1.0 | 111.5±2.1 | 5.4±3.5 | -55.7±3.3 |
| D_20 | 143.4±2.7 | 4.7±1.8 | -44.0±2.1 | 137.8±3.8 | 9.8±4.4 | -47.0±3.6 |
| D_30 | 96.4±2.0 | 2.5±1.6 | -44.8±2.1 | 98.6±4.0 | 12.7±6.1 | -63.5±6.5 |
| S_0 | 127.4±4.1 | 4.1±3.1 | -45.2±1.1 | 135.7±2.8 | 5.7±5.2 | -42.2±1.2 |
| S_10 | 132.3±3.2 | 3.9±3.0 | -45.2±0.9 | 142.1±1.9 | 2.5±2.1 | -38.4±0.4 |
| S_20 | 113.4±2.1 | 3.7±2.5 | -46.2±5.2 | 119.0±6.6 | 8.4±9.0 | -45.7±3.9 |
| S_30 | 109.0±1.7 | 4.2±2.8 | -53.1±4.0 | 105.8±1.4 | 5.5±2.5 | -50.2±2.6 |

The influence of $CaCl_2$ electrolyte solutions with different concentrations on the stability of latexes was monitored (see **Table 10**). It was shown that the D_20 sample showed the greatest stability towards the $CaCl_2$ electrolyte. No clear connection was demonstrated when comparing the influence of the emulsifiers used on the electrolytic stability of latexes towards divalent ions. The mechanical and heat stability results (see **Table 10**) proved that both the emulsifiers and the bio-based content did not affect the stability of the latexes produced.

Regarding the freeze-thaw stability (see **Table 10**), it was shown that all samples were stable at a temperature of −5 °C. The latexes of the D-series were not stable at a temperature of −10 °C except the D_10. Latexes of the S-series were found stable at −10 °C except the S-30. It was noticed that up to 20 wt.% of the bio-based monomer content in the S-series the latexes could withstand a temperature of −10 °C. However, at a lower temperature (−18 °C), destabilization and subsequent coagulation of polymer particles occurred already after the first freeze-thaw cycle.

**Table 10**. Results of stability testing of latex samples regarding resistance to $CaCl_2$, mechanical stability, heat storage stability, and freeze-thaw stability

| Sample name | Concentration of $CaCl_2$ (wt. %) | | | | | | | | | Mechanical stability | Heat storage stability +60 °C | Freeze-thaw stability | | |
|---|---|---|---|---|---|---|---|---|---|---|---|---|---|---|
| | 0.01 | 0.05 | 0.1 | 0.2 | 0.5 | 1.0 | 1.5 | 2.0 | 5.0 | | | –5 °C | –10 °C | –18 °C |
| D_0 | √ | √ | √ | √ | √ | √ | √ | √ | – | √ | √ | √ | – | – |
| D_10 | √ | √ | √ | √ | √ | √ | √ | √ | – | √ | √ | √ | √ | – |
| D_20 | √ | √ | √ | √ | √ | √ | √ | √ | √ | √ | √ | √ | – | – |
| D_30 | √ | √ | √ | √ | √ | √ | √ | √ | – | √ | √ | √ | – | – |
| S_0 | √ | √ | √ | √ | √ | √ | √ | √ | – | √ | √ | √ | √ | – |
| S_10 | √ | √ | √ | √ | √ | √ | √ | √ | – | √ | √ | √ | √ | – |
| S_20 | √ | √ | √ | √ | √ | √ | √ | √ | – | √ | √ | √ | √ | – |
| S_30 | √ | √ | √ | √ | √ | √ | √ | √ | – | √ | √ | √ | – | – |

Stability results expressed by symbols: "√" means no visible coagulation, "–" means visible coagulation.

## 3.3. Characterization of copolymer structure by IR spectroscopy

The structure of latex copolymers and the content of incorporated bio-based building blocks in the polymer backbone were followed by IR spectroscopy. For both series of latex copolymers, similar IR spectra for the corresponding concentrations of the bio-based monomer in the copolymer were obtained (**Figs. 9** and **10**). All the spectra exhibited a weak absorption band at 620 $cm^{-1}$, which is characteristic of sulfate groups ($SO_4^{2-}$) and indicates the employment of both emulsifiers. The spectra of all the copolymers further showed absorption bands at 2963 and 2866 $cm^{-1}$ corresponding to asymmetric and symmetric vibrations of the $CH_3$ group, a weak absorption band at 2928 $cm^{-1}$, which could be assigned to vibrations of the $CH_2$ group, and a strong absorption band of the C=O group at 1728 $cm^{-1}$, which is characteristic of the carboxylic acid ester group. The copolymerization of DAAM was evidenced by the absorption band at 1535 $cm^{-1}$, which could be assigned to the N–H bond. All the copolymers also exhibited a weak absorption band at 1640 $cm^{-1}$ corresponding to the N=C bond, which proved that the keto-hydrazide reaction occurred in the coating films. **Figures 11** and **12** document in more detail the increasing intensity of CH stretching

bands of methylene groups at 2931 and 2855 $cm^{-1}$, which correlates well with the increasing content of the bio-based monomer used for the synthesis of latexes. This feature verifies the successful incorporation of vegetable oil-based building blocks into the polymer structure.

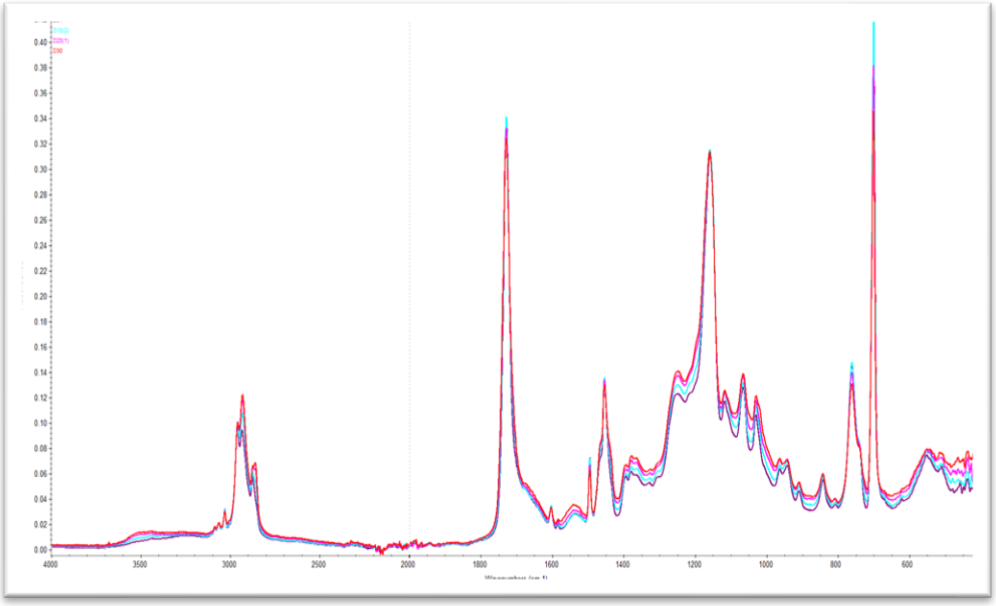

**Figure 9**. IR spectra of copolymers comprising Disponil FES 993 emulsifier: D_0 (violet), D_10 (cyan), D_20 (magenta) and D_30 (red).

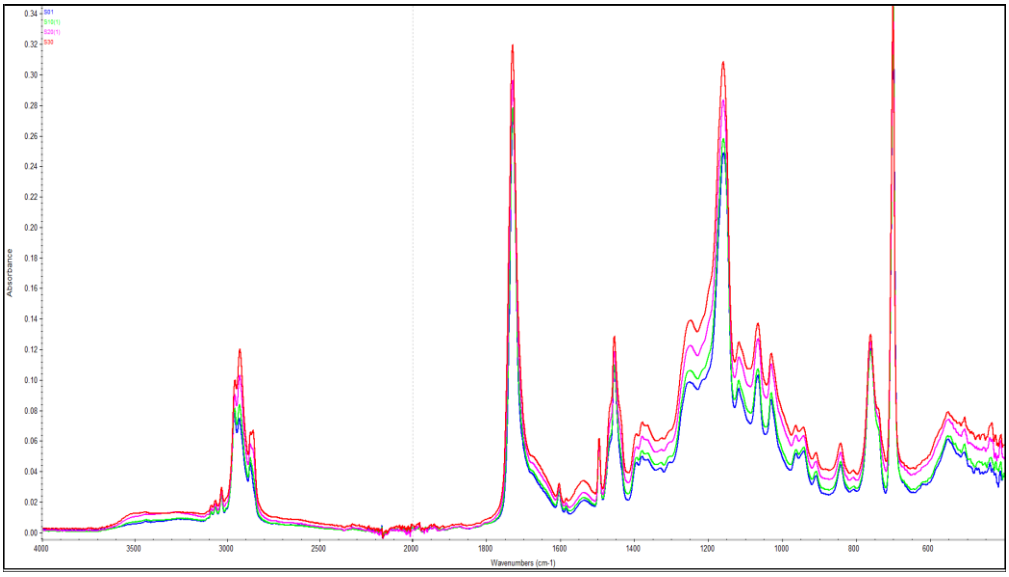


**Figure 10**. IR spectra of copolymers comprising SR-10 emulsifier: S_0 (blue), S_10 (green), S_20 (pink) and S_30 (red).

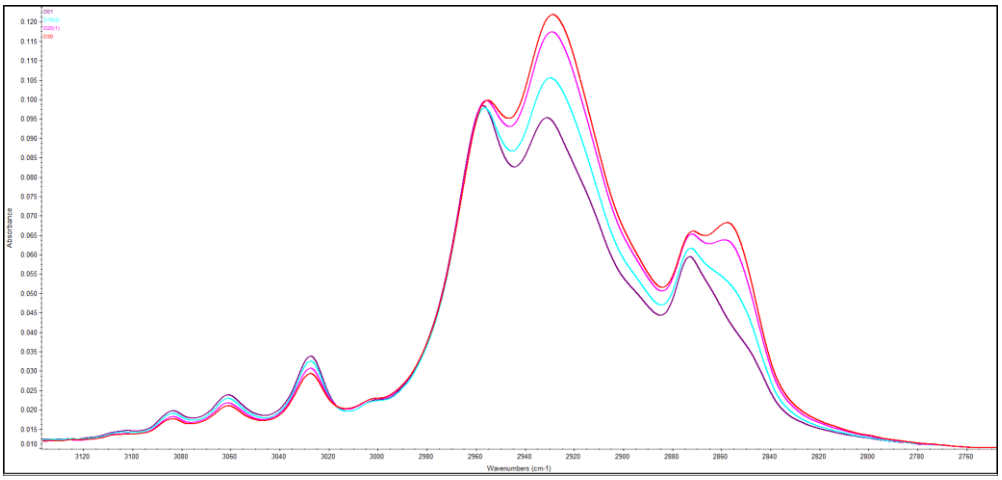


**Figure 11**. Detailed IR spectra of copolymers comprising Disponil FES 993 emulsifier: D_0 (violet), D_10 (cyan), D_20 (magenta) and D_30 (red).

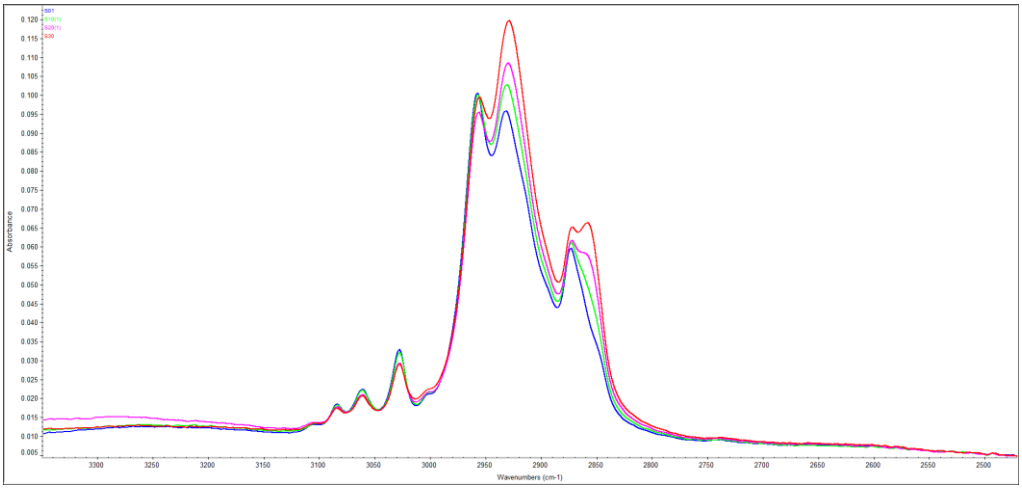


**Figure 12**. Detailed IR spectra of copolymers comprising SR-10 emulsifier: S_0 (blue), S_10 (green), S_20 (pink) and S_30 (red).

## 3.4. Characterization of molar mass distribution by AF4-MALS

Most of the analyzed samples have bimodal molar mass distribution where the first peak at lower retention times corresponds to dissolved macromolecules and the second peak at higher retention times belongs to crosslinked latex particles (nanogels). The molar mass characteristics are summarized in **Table 11,** which lists the following quantities: weight fractions of polymer and

nanogels, the weight-average molar mass ($M_w$) and polydispersity (the ratio of the weight-average and number-average molar mass, $M_w/M_n$) are used to characterize polymer fraction, the values of $M_w$ and *z*-average root mean square (RMS) radius (radius of gyration) are used to characterize the nanogel fraction. Polydispersity for nanogels was in all cases close to unity. However, it is unclear whether nanogels are monodisperse or if the AF4 technique cannot separate them.

**Figures 13** and **14** show two examples of typical fractograms and molar mass versus retention time plots for continuous molar mass distribution (samples without nanogels); the same plots for bimodal distribution (samples containing nanogels) are depicted in **Figures 15** and **16**.

**Table 11**. Molar mass characteristics of latex copolymers

| Sample | Polymer | | | Nanogel | | |
|---|---|---|---|---|---|---|
| | $M_w$ ($10^3$ g/mol) | $M_w/M_n$ | Fraction (%) | $M_w$ ($10^6$ g/mol) | Fraction (%) | $R_z$ (nm) |
| D_0 | 320 | 4.1 | 100 | – | – | – |
| D_10 | 568 | 9.4 | 81 | 67 | 19 | 118 |
| D_20 | 341 | 6.3 | 76 | 111 | 24 | 135 |
| D_30 | 72 | 2.0 | 30 | 126 | 70 | 83 |
| S_0 | 431 | 3.8 | 100 | – | – | – |
| S_10 | 308 | 4.2 | 52 | 304 | 48 | 134 |
| S_20 | 267 | 5.3 | 58 | 106 | 42 | 104 |
| S_30 | 86 | 2.3 | 34 | 168 | 66 | 83 |

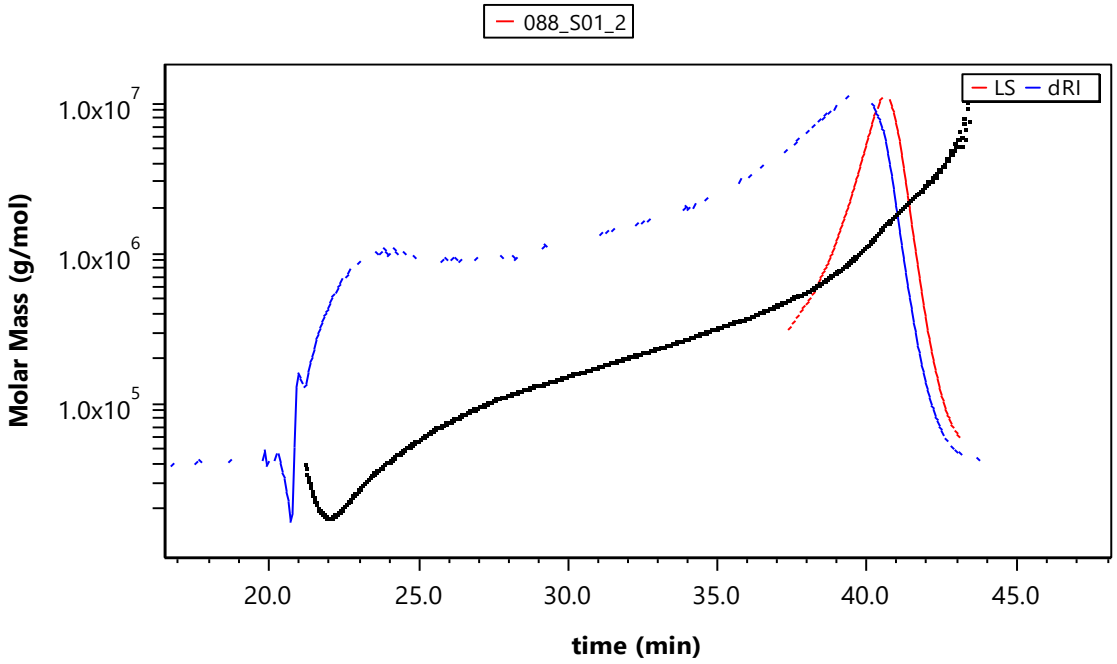


**Figure 13**. Molar mass versus retention time plots for sample S_0 with unimodal molar mass distribution. The signals of RI (blue) and MALS @90°detectors are overlaid here.

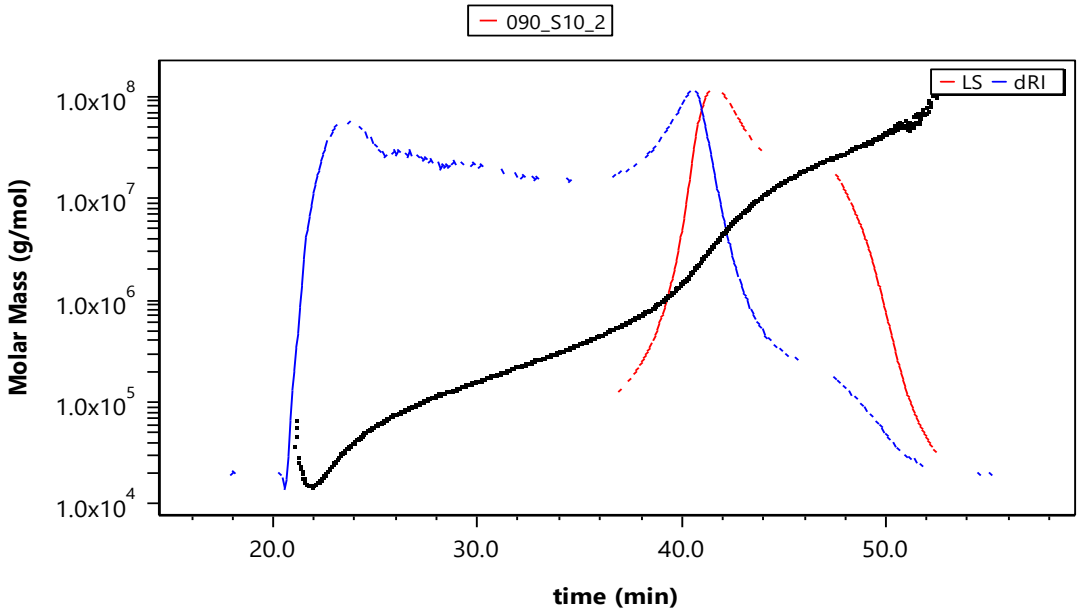


**Figure 14**. Molar mass versus retention time plots for sample S_10 with unimodal molar mass distribution: The signals of RI (blue) and MALS @90°detectors are overlaid here.

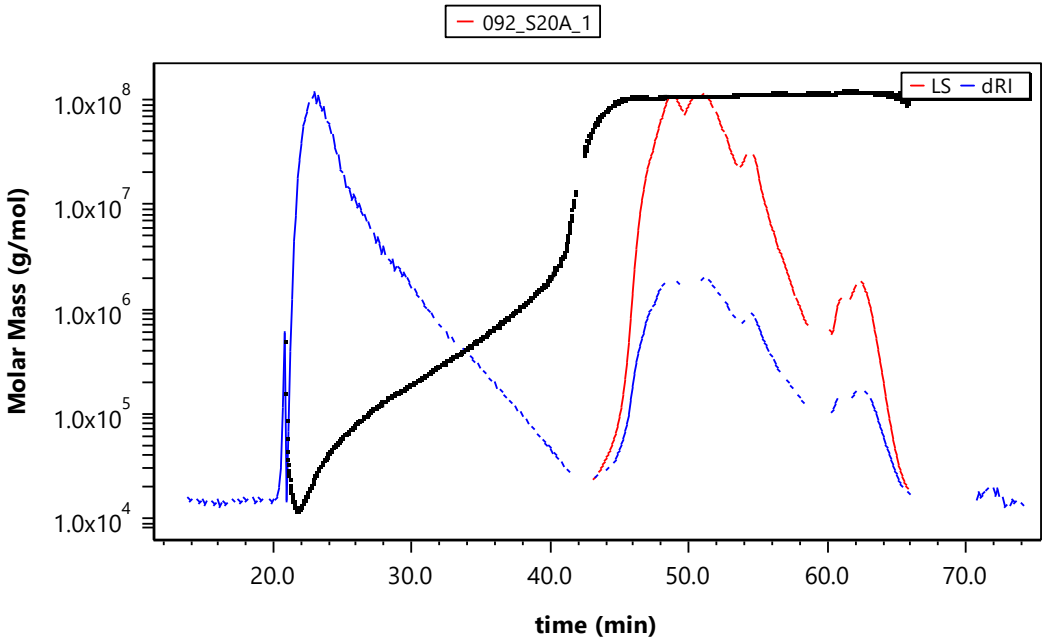


**Figure 15**. Molar mass versus retention time plots for sample S_20 with bimodal molar mass distribution containing nanogels. The signals of RI (blue) and MALS @90°REDdetectors are overlaid here.

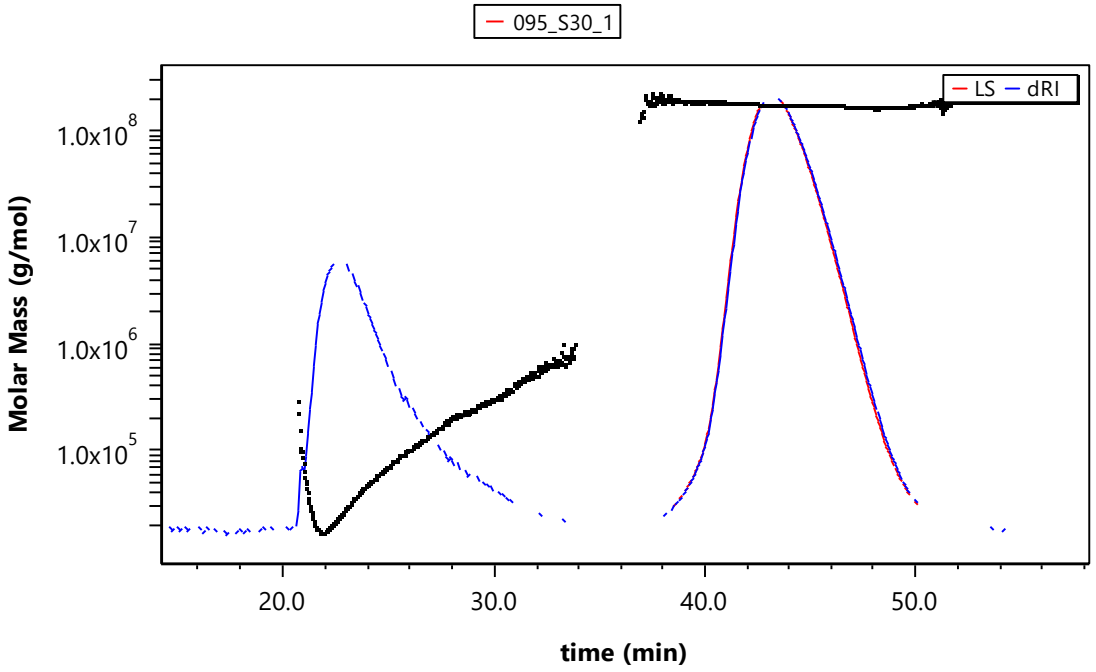


**Figure 15**. Molar mass versus retention time plots for sample S_30 with bimodal molar mass distribution containing nanogels. The signals of RI (blue) and MALS @90°REDdetectors are overlaid here.

## 3.5. Determination of MFFT and Tg

To evaluate the properties of the latexes regarding their applicability in coating applications, it is necessary to determine MFFT and/or $T_g$, which are given in **Table 12**. It was shown that for the $T_g$ values the higher the bio-based monomer content, the lower the $T_g$. This fact indicates the plasticizing effect of the copolymerized sunflower oil-based monomer. The heat capacity ($c_p$) exhibited standard values that are typical for the glass transition of polymers. The plasticizing effect of the introduced bio-monomer was also demonstrated in the case of MMFT values. In addition, it can be concluded that all the MFFT values of the samples were sufficiently low, indicating excellent film-forming properties.

**Table 12**. Values of minimum film-forming temperature and glass transition temperature for all types of latex samples

| Sample name | $T_g$ (°C) | $c_p$ (J/g·°C) | MFFT(°C) |
|---|---|---|---|
| D_0 | 18.4±0.1 | 0.3±0.1 | 13.5 |
| D_10 | 11.1±13.0 | 0.3±0.3 | 6.4 |
| D_20 | -0.2±9.3 | 0.3±0.3 | <0 |
| D_30 | 1.3±0.8 | 0.3±0.0 | <0 |
| S_0 | 21.2±0.9 | 0.3±0.0 | 12.4 |
| S_10 | 12.2±3.3 | 12.2±0.0 | 3.5 |
| S_20 | 0.9±0.7 | 0.3±0.0 | <0 |
| S_30 | -3.0±0.0 | 0.3±0.0 | <0 |

## 3.6. Determination of gel content and crosslink density of latex materials

To investigate the effects of the bio-monomer content and emulsifier type on the structure of the prepared latex samples from the point of view of cross-linking, the gel content, and the corresponding extractable fraction, which expresses the percentage of unembedded macromolecular chains in the polymer system, were determined. The average molar mass $M_c$, which corresponds to the polymer chain between two cross-linking nodes in the polymer network, and the network density were also calculated (see **Table 13)**.

In the case of D_ 0 and S_ 0 latex materials, it was experimentally demonstrated that the gel content values were lower in the case of D-series. The lowest value was determined for the sample D_0, where no bio-based monomer was used. On the other hand, the highest gel content value was

obtained for the S_10 sample, using a polymerizable emulsifier. From the experimentally determined values, the emulsion copolymers prepared with a polymerizable emulsifier have a higher gel content. At the same time, it has been confirmed that the higher the gel content of the given system, the higher its crosslink density. Therefore, it can be stated that the experimentally determined results of measuring the gel content and the crosslink density of the prepared samples of emulsion copolymers are correlated Regarding the results of crosslink density, it can be stated for both series of latex polymers that the higher the bio-monomer content the higher the crosslink density. This phenomenon can be explained by the branching ability of the sunflower oil-based bio-monomer, which probably resulted in nanogel formation (confirmed by A4F-MALS, see **Figures 15** and **16**).

**Table 13**. Evaluation of latex materials in terms of gel content and crosslink density

| Sample | Gel content (wt.%) | Crosslink density ($\times 10^{-6}$ mol nodes/cm$^3$ | $M_c$ (g/mol) |
|---|---|---|---|
| D_0 | 57.64 | 2.89±0.15 | 373,000±19,100 |
| D_10 | 70.00 | 6.11±0.71 | 184,000±21,200 |
| D_20 | 73.38 | 13.80±2.26 | 82,000±13,500 |
| D_30 | 82.79 | 33.90±3.30 | 33,000±3,300 |
| S_0 | 65.16 | 5.99±0.71 | 187,000±22,100 |
| S_10 | 83.92 | 15.80±6.61 | 71,000±3,000 |
| S_20 | 78.46 | 17.56±1.28 | 64,000±4,700 |
| S_30 | 75.02 | 38.51±1.85 | 29,000±1,400 |

## 3.7. Determination of water absorption

This experiment was carried out to determine the sensitivity of the coating film to the action of water. The absorbency of latex samples exposed to water for 30 days was determined. During this time, weight gain was measured after 1, 4, 5, 7, 14, and 30 days; a detailed analysis of the course of absorption of the latex on individual days is recorded in **Figures 16** and **17.** In **Figure 16**, D-series latexes differing from the bio-based monomer content are compared over time. There was a linear increase from initial days (1 – 4) and a sharp decrease in the D_ 0 sample from day 5 to day 30. The D_ 10 sample exhibited increased water absorption from day 5 to 7 and steadily decreased water absorption from day 14 to day 30. There was unusual behavior in the D_ 20 sample; there

was no evidential absorption from initial days (1 – 7), and sharply absorbed water from day 14 to day 30, the highest absorption among the series. There was a clear linear increase in water absorption in the S- series. The S_10 sample absorbed the most water over time, followed by the S_30 sample as shown in **Figure 17.**

**Figure 18** compares the water absorption capacity regarding the type of emulsifier used and the amount of bio-based monomer incorporated in the latex copolymer. In all cases, samples with the polymerizable (SR-10) emulsifier absorbed more water than those with the non-polymerizable (Disponil FES 993) emulsifier. In both series, the higher the amount of bio-based monomer, the higher the water absorption rate, except for the S_20 sample. It is evident from the experimental data that the bio-based monomer incorporated and polymerizable emulsifier used contributed to the high rate of water absorption. Therefore, it is recommended that latexes where water resistivity property is paramount should be prepared using a non-polymerizable emulsifier.

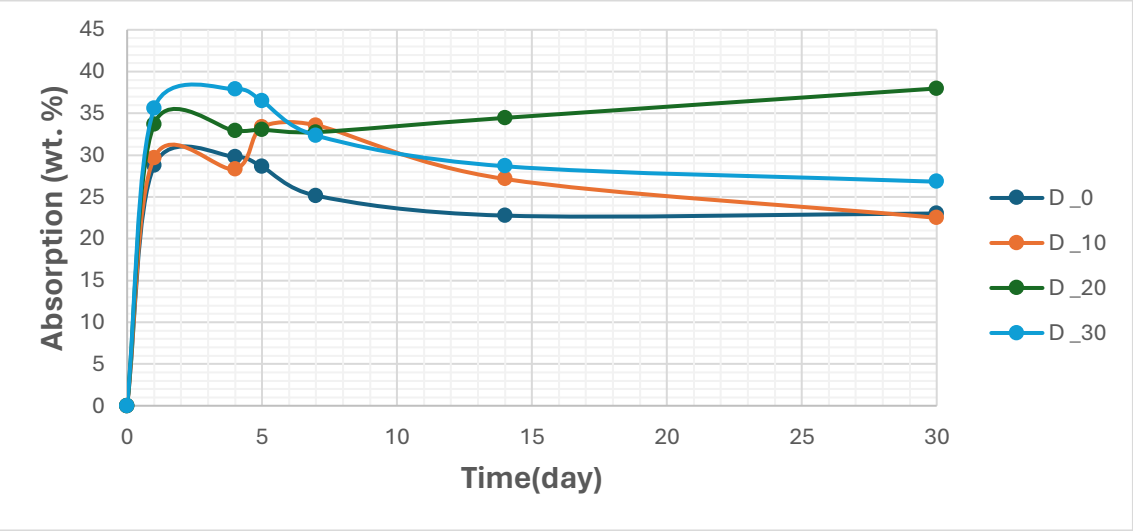


**Figure 16**. Comparison of water absorbed by the film for D-series of latexes during 30 days of water exposure.

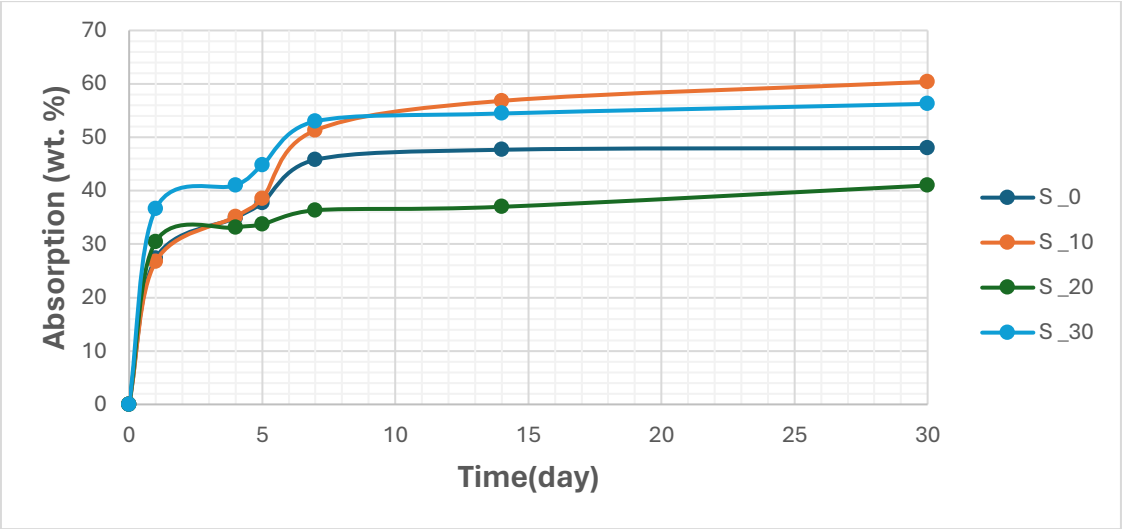


**Figure 17**. Comparison of water absorbed by the film for S-series of latexes during 30 days of water exposure.

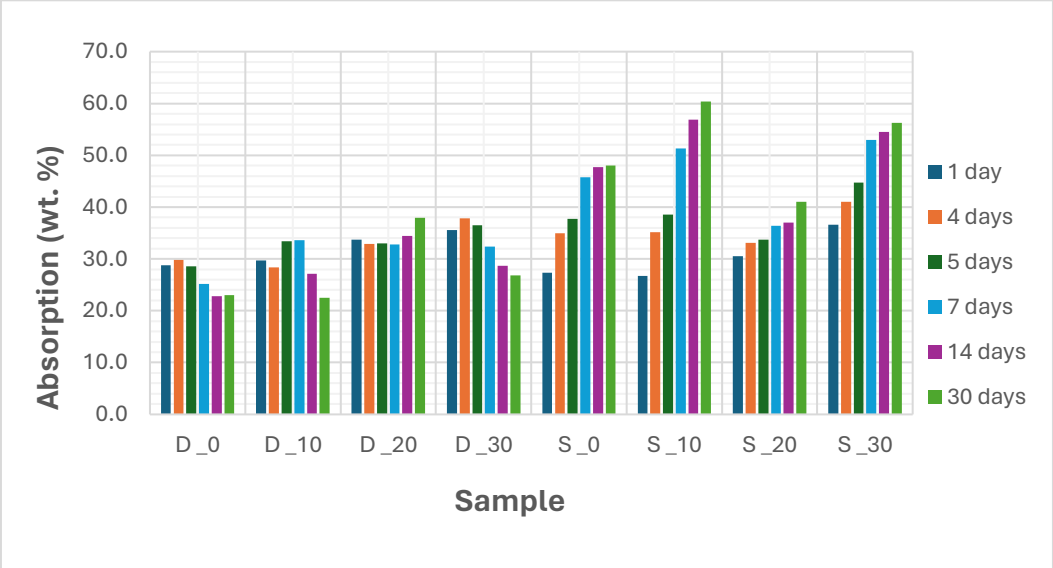


**Figure 18**. Comparison of latex films in terms of their water absorption (amount of water absorbed by the film).

## 3.8. Determination of hardness

According to Persoz, hardness measurement was used to determine the mechanical resistance of coat films depending on the type of emulsifier used and the amount of bio-based monomer. In **Table 14**, the average values of the relative hardness of the individual samples determined after 7

days are recorded. Other results documenting the evolution of coating hardness over time were not recorded in the table due to almost unchanged values during further measurements. The results showed that the higher the bio-monomer content, the lower the hardness, which reveals again the plasticizing effect of the sunflower oil-based monomer. In addition, the type of emulsifier used wasn´t found to provide any significant effect on coating hardness.

Various pencils of different hardness were used to assess the surface hardness of the coating films. The experiment's objective was to identify the initial irreversible damage to the film because of the pointed tip of the pencil. The results of the pencil scratch test, summarized in **Table 13**, confirm the plasticizing effect of the bio-monomer in the D-series of latex films. While the influence of the surfactant in determining the final surface hardness was inconclusive, the polymerizable surfactant SR-10 exhibited a "self-healing" effect in the dispersions. This phenomenon, which leads to the restoration of damaged coatings, can be explained as follows: Mechanical force induced reversible deformation and disruption of physical bonds on the film surface formed by latex particles containing covalently bound surfactant, which were subsequently restored after the force was removed. Conversely, in films formed by latex particles surrounded by physically bound surfactant molecules, mechanical damage appeared to result in their irreversible removal and destruction of the resulting film structure.

**Table 14**. shows the results of pendulum hardness, pencil hardness, cross-cut test, and pull-off test of latex on a glass substrate.

| Sample name | Pendulum hardness | Pencil hardness (type/number of pencil) | Cross-cut test | Pull-off test (MPa) |
|---|---|---|---|---|
| D_0 | 33.7±0.6 | 5F/5 | 0 | 5.3±1.9 |
| D_10 | 12.7±0.1 | 4HB/4 | 0 | 6.3±0.9 |
| D_20 | 5.4±0.0 | 4HB/4 | 0 | 3.9±0.2 |
| D_30 | 6.2±0.1 | 4HB/4 | 0 | 4.1±0.7 |
| S_0 | 34.9±0.0 | 3B/3 | 0 | 5.7±2.2 |
| S_10 | 16.4±0.1 | 3B/3 | 0 | 5.9±0.2 |
| S_20 | 4.9±0.2 | 4HB/4 | 0 | 3.5±0.6 |
| S_30 | 6.3±0.3 | 4HB/4 | 0 | 3.8±0.1 |

## 3.9. Determination of adhesion

The results of the pull-off test, which indicate the degree of adhesion of latex films to the glass substrate, are shown in **Table 14** The values show high adhesion of all films. It was noticed that the type of emulsifier used did not show any evidential difference. It was also noticed that the samples D_10 and S_10 (synthesized using 10 wt. % of the bio-based monomer) exhibited the highest adhesion in the respective series.

Also included in **Table 14** are the results of the adhesion properties of the latex films monitored using the cross-cut test. As can be seen from the comparison of both methods, the results correlate and, therefore, support the hypothesis described in the previous pull-off test. Thus, there was no evidential difference between the type of emulsifier used and the bio-based monomer incorporated.

## 3.10. Determination of gloss

**Table 15** shows the gloss values of the coatings, measured at an angle of 60°. The results showed that, except for the D_ 0 and S_0 samples, all realized coatings of the tested dispersions stand out with good gloss. The result showed that coatings with bio-based monomers had a better gloss than those without bio-based monomers, except for S_10. D-series samples exhibited higher gloss than those of S-series.

Latexes were also tested for their ability to provide coatings with retained gloss, even during prolonged exposure to elevated temperatures (60 °C). It turned out that the dispersions of both series were stable even outside the standard conditions and provided smooth and continuous coating films. There was an improvement in the gloss, regardless of the type of emulsifier and amount of bio-based monomer used. This is because latex particles coalesce more efficiently at elevated temperatures, forming a continuous film with smoother surfaces. This enhances light reflection and results in a glossy appearance. Also, heating latex polymers increases their chain mobility, promoting molecular rearrangement and alignment at the surface; this alignment enhances light reflection and glossiness. The latexes were also examined from the point of view of storing below 0 °C. In case the latex retained the colloidal stability, the respective coating film exhibited higher gloss.

**Table 15**. Gloss of latex films cast from original latex samples, films cast from latex samples subjected to heat storage testing, and films cast from latex samples subjected to freeze-thaw testing at −5 °C, −10 °C, and −18 °C.

| Sample name | Original state (GU) | After heat storage test (GU) | After freeze-thaw (GU) | | |
|---|---|---|---|---|---|
| | | | −5°C | −10°C | −18°C |
| D_0 | 30.1±0.4 | 42.7±1.8 | 32.1±0.2 | – | – |
| D_10 | 82.5±1.1 | 91.7±1.9 | 91.0±2.6 | 91.0±3.0 | – |
| D_20 | 61.4±5.6 | 81.4±4.0 | 77.9±2.2 | – | – |
| D_30 | 78.1±0.8 | 69.4±2.4 | 80.6±4.1 | – | – |
| S_0 | 30.4±1.4 | 35.6±3.6 | 36.8±1.8 | 92.6±0.5 | - |
| S_10 | 36.3±0.2 | 40.2±1.2 | 47.9±5.2 | 47.5±4.2 | – |
| S_20 | 61.2±2.1 | 78.0±0.7 | 48.5±2.0 | 52.3±1.2 | – |
| S_30 | 72.3±1.4 | 77.1±3.8 | 79.8±3.8 | – | – |

"–" Means visible coagulation.

## 3.11. Determination of resistance to methyl ethyl ketone

This test was performed to determine the chemical resistance of latex films to a polar organic solvent. **Table 16** shows the results of the measurements. It was found that coatings of both series did not resist the polar organic solvent used. However, the S-series coatings exhibited improved MEK resistance compared to the D-series coatings. The results showed that a high percentage of bio-based monomer incorporated contributed to better MEK resistance of coatings in both series. This may be because of their functional groups and molecular structure.

**Table 16**. Results show the resistance of latex films to methyl ethyl ketone for individual dispersions.

| Sample name | MEK resistance (s) |
|---|---|
| D_0 | 6.7±1.2 |
| D_10 | 3.0±0.0 |
| D_20 | 3.9±1.0 |
| D_30 | 8.3±2.3 |
| S_0 | 9.2±1.0 |
| S_10 | 11±1.0 |
| S_20 | 6.0±2.6 |
| S_30 | 8.0±1.0 |

## 3.12. Determination of water whitening

The resistance of latex coating films to water penetration, which results from preventing water transport into the interstitial spaces and internal structure of the latex film, was tested. This evaluation assessed the resulting turbidity intensity after exposing the samples to distilled water for 1, 4, and 24 h. The increase in opacity or whitening of the coating film was evaluated by measuring the transmittance. The percentage decrease in this parameter signifies the degree of whitening of the coating (*W*) and indicates an increased susceptibility of latex coating films to water. This susceptibility not only predisposes the film to potential damage due to swelling but also reduces the visual appeal of the coating material.

In **Figures 20** and **21**, it was demonstrated that the higher the content of the bio-based monomer incorporated, the lower the whitening over time. The exceptions represent only the samples D_10 and S_10, providing coating films with increased whitening in comparison with the respective reference coatings (without the bio-monomer introduced). It was also found that latexes with the polymerizable emulsifier showed a better whitening resistance than non-polymerizable emulsifier-based latexes. In the S_0 sample, whitening reduces over time, while in the D_0 sample, it increases over time. From the result, the emulsifier type significantly affected the coat film's whitening level. Both emulsifiers and bio-based monomers affected the whitening of the latexes. As in the case of determining the absorption values described in the previous chapter, 3.3.6.1, the significant effect

of the type of emulsifier used and the amount of bio-based monomer incorporated was again demonstrated.

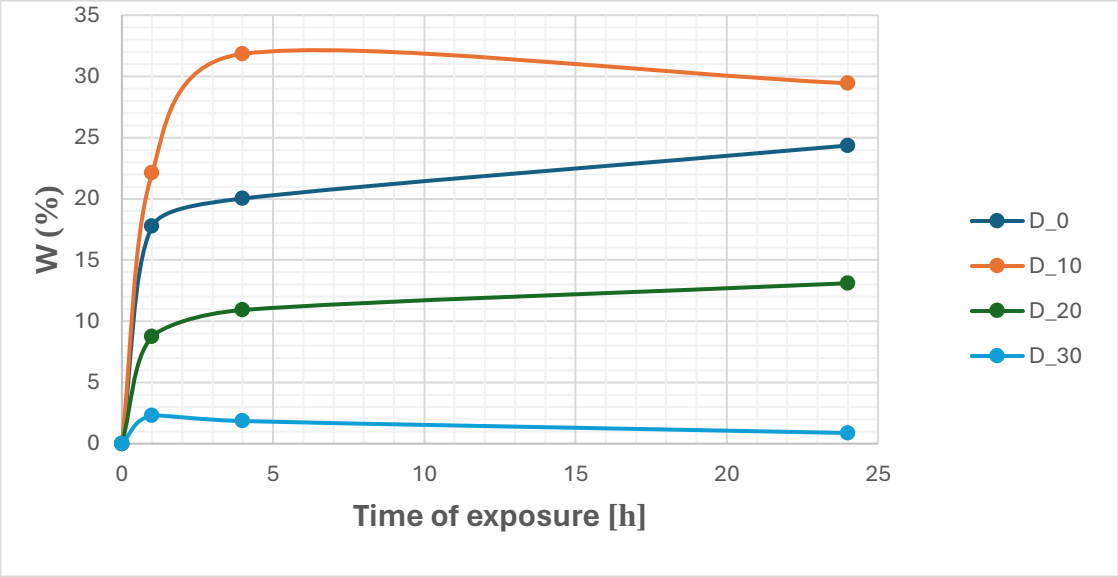


**Figure 19**. Graphical dependence of whitening of D-series coat films on water exposure time.

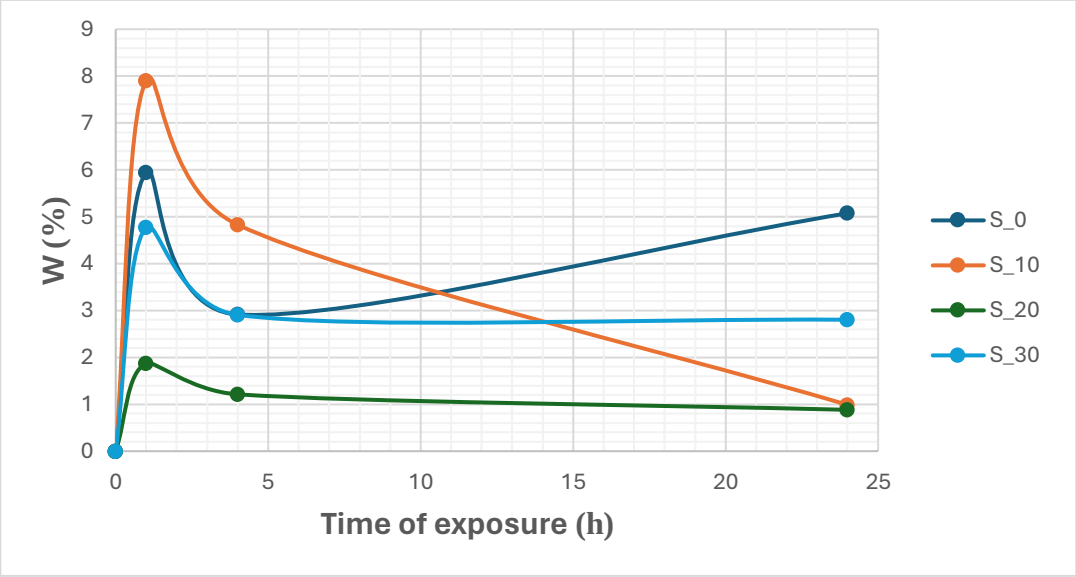


**Figure 20**. Graphical dependence of whitening of S-series coat films on water exposure time.

## 3.13. Determination of surface properties

In this experimental part of the work, it was crucial to assess whether the coating film wets due to the action of the aqueous environment on the material with the given latex or, on the contrary, the wettability does not occur, and whether the results correlate with previous methods, which also touched on the issue of the sensitivity of coating films to water (see chapters 3.3.10). The determination was made through a drop of water that was placed on a glass slide with a dry coating film, and the size of the contact angle for water was determined using a tensiometer. It was also necessary to determine the size of the contact angle for diiodomethane. Diiodomethane is often used as a non-polar liquid for contact angle measurements because it does not mix with water and forms a clear interface with it, which was important from the point of view of determining the surface energy of the given latex coating. The contact angles and the calculated values of the surface energy of the respective latex film are given in **Table 17.** It is clear from the results that the larger the size of the contact angle, the lower the value of the surface energy of the latex, and the liquid thus poorly wets the surface of the coat films. The lowest surface energy values have the coatings that contain no copolymerized bio-based monomer. A comparison of the sizes of the contact angles for water and the sizes of the surface energies of individual samples in both emulsifiers did not consist of the same. So, it was difficult to ascertain the level of effect of emulsifiers on the surface energy. From a general point of view, it is not possible to unequivocally state an improvement in the material's resistance due to the type of emulsifier used.

**Table 17**. Values of the contact angle for water and diiodomethane, including calculated surface free energy values for the latexes.

| Sample Name | Water contact angle (°) | Diiodomethane contact angle (°) | Surface free energy (mN/m) |
|---|---|---|---|
| D_0 | 92.4±1.4 | 83.3±3.2 | 18.4±1.0 |
| D_10 | 78.3±1.5 | 59.7±2.0 | 31.0±0.8 |
| D_20 | 66.3±7.2 | 49.6±6.4 | 29.7±4.0 |
| D_30 | 92.2±0.7 | 73.0±12.2 | 22.4±4.9 |
| S_0 | 84.6±2.2 | 74.1±7.9 | 24.4±2.4 |
| S_10 | 81.1±8.1 | 66.3±10.5 | 28.2±6.6 |
| S_20 | 90.9±0.6 | 91.3±1.2 | 16.1±3.2 |
| S_30 | 87.1±0.7 | 56.8±6.2 | 31.2±2.0 |

## 3.14. Evaluation of mechanical properties of coat films on a steel substrate

It is evident from **Table 19** that the mechanical properties of the coating films were not affected by the type of emulsifier used and the amount of bio-based monomer incorporated during the synthesis. Latex films on steel panels withstood a weight drop from a height of 100 cm, body indentation to a depth of 10 mm, and bending on a 2 mm diameter mandrel.

This was the maximum load for all the mentioned tests. Therefore, the coatings did not lose cohesion and adhesion to the substrate and achieved excellent resistance to impact deformation.

Determination of adhesion of the coat films was evaluated for a steel substrate. From **Table 19,** it was clear that all coatings showed the maximum degree of adhesion according to the grid test, therefore it was evident that a stronger adhesion to the surface was achieved when applied to steel substrate. A pull-off test was performed on the coat films on steel substrate according to the procedure in chapter, 2.3.16. from the results, there was no significant difference between the type of emulsifier used. It was clear that the bio-based monomer did not influence the adhesion property of the coat films.

**Table 17**. The results of the cupping test, impact test, bending test, adhesion cross-cut test, and pull-off test for the coating on a steel substrate.

| Sample name | Cupping test (mL) | Bending test | Adhesion cross-cut test (ISO) | Pull-off test |
|---|---|---|---|---|
| D_0 | >10 | <2 | 0 | 0.4±0.6 |
| D_10 | >10 | <2 | 0 | 1.1±0.6 |
| D_20 | >10 | <2 | 0 | 1.0±0.2 |
| D_30 | >10 | <2 | 0 | 1.7±0.2 |
| S_0 | >10 | <2 | 0 | 1.1±0.6 |
| S_10 | >10 | <2 | 0 | 1.8±0.8 |
| S_20 | >10 | <2 | 0 | 1.1±0.6 |
| S_30 | >10 | <2 | 0 | 1.6±0.3 |

# CONCLUSION

Acrylated methyl ester of sunflower oil was copolymerized with standard petroleum-based acrylate monomers using semi-continuous emulsion polymerization, resulting in two sets of film-forming polymer latexes with different anionic emulsifier types, namely, polymerizable emulsifier (SR-10) and non-polymerizable emulsifier (Disponil FES 993). Successful emulsion polymerization was achieved with both emulsifier types, with conversions reaching approximately 95% and coagulum content remaining below 3% for bio-based derivative concentrations of up to 30 wt.% in the monomer blend. Including 30 wt.% of the bio-based monomer did not affect the storage, electrolytic, and mechanical stability of the latexes.

The successful copolymerization of the bio-based monomer was proved by IR spectroscopy and by A4F-MALS technique. The latter method revealed branching and crossing-linking in the structure of copolymers comprising the bio monomer. The phenomenon of cross-linking and extensive branching was more distinctive in the latexes with the increasing content of bio-based monomer incorporated. Important also was the effect of plasticization due to the bio-based monomer copolymerization that resulted in a decrease in $T_g$ and MFFT.

Latexes synthesized using the polymerizable emulsifier with a high bio-based monomer content provided enhanced water resistance than the latexes prepared using the non-polymerizable emulsifier. The aspect of sustainability supported by the improved water resistance of the latexes prepared using the polymerizable emulsifier makes these latexes suitable for protection of various substrates suspected to humid areas. Therefore, the latexes produced using the sunflower oil-based derivative seem to be suitable for replacing traditional petroleum-based products in the coating industry. Materials with a high degree of cross-linking and containing the polymerizable emulsifier SR-10 show excellent properties that make them suitable also for printing inks and adhesives.

# REFERENCES


[1] E. Nekhavhambe, H. E. Mukaya, and D. B. Nkazi, “Development of castor oil–based polymers: A review,” *J Adv Manuf Process*, vol. 1, no. 4, Oct. 2019, doi: 10.1002/amp2.10030.

[2] G. Çayli, D. Gürbüz, and A. Çınarli, “Characterization and Polymerization of Epoxidized Methacrylated Castor Oil,” *European Journal of Lipid Science and Technology*, vol. 121, no. 1, Jan. 2019, doi: 10.1002/ejlt.201700189.

[3] A. N. M. B. El-hoshoudy, “Emulsion Polymerization Mechanism,” in *Recent Research in Polymerization*, InTech, 2018. doi: 10.5772/intechopen.72143.

[4] M. Kolář *et al.*, “Derivatives of linseed oil and camelina oil as monomers for emulsion polymerization,” *J Mater Sci*, vol. 58, no. 39, pp. 15558–15575, Oct. 2023, doi: 10.1007/s10853-023-08969-4.

[5] C. S. Chern, “Emulsion polymerization mechanisms and kinetics,” *Prog Polym Sci*, vol. 31, no. 5, pp. 443–486, May 2006, doi: 10.1016/j.progpolymsci.2006.02.001.

[6] “Odian G. Emulsion polymerization,Principles of polymerization. Fourth edition John Wiley & Sons, Inc; 2004:350-371”.

[7] “Schild HG. Poly (N-isopropylacrylamide): Experiment, theory and application. Progress in Polymer Science. 1992;17(2):163-249”.

[8] Y. H. Ho, A. Parthiban, M. C. Thian, Z. H. Ban, and P. Siwayanan, “Acrylated Biopolymers Derived via Epoxidation and Subsequent Acrylation of Vegetable Oils,” *International Journal of Polymer Science*, vol. 2022. Hindawi Limited, 2022. doi: 10.1155/2022/6210128.

[9] L. M. De Espinosa, J. C. Ronda, M. Galià, and V. Cádiz, “A new route to acrylate oils: Crosslinking and properties of acrylate triglycerides from high oleic sunflower oil,” *J Polym Sci A Polym Chem*, vol. 47, no. 4, pp. 1159–1167, Feb. 2009, doi: 10.1002/pola.23225.

[10] M. Alam, D. Akram, E. Sharmin, F. Zafar, and S. Ahmad, “Vegetable oil based eco-friendly coating materials: A review article,” *Arabian Journal of Chemistry*, vol. 7, no. 4. Elsevier, pp. 469–479, 2014. doi: 10.1016/j.arabjc.2013.12.023.

[11] “A. M. Diez-Pascual, ‘Antibacterial nanocomposites based on thermosetting polymers derived from vegetable oils and metal oxide nanoparticles,’ Polymers, vol. 11, no. 11, p. 1790, 2019”.

[12] “G. Lligadas, J. C. Ronda, M. Galià, and V. Cádiz, ‘Renewable polymeric materials from vegetable oils: a perspective,’ Mate- rials Today, vol. 16, no. 9, pp. 337–343, 2013.”.

[13] “Emulsion Polymerization,” in *Principles of Polymerization*, Wiley, 2004, pp. 350–371. doi: 10.1002/047147875X.ch4.

[14] W. D. Harkins, “A General Theory of the Mechanism of Emulsion Polymerization [1],” *J Am Chem Soc*, vol. 69, no. 6, pp. 1428–1444, Jun. 1947, doi: 10.1021/ja01198a053.

[15] J. M. Asua, “Emulsion polymerization: From fundamental mechanisms to process developments,” *J Polym Sci A Polym Chem*, vol. 42, no. 5, pp. 1025–1041, Mar. 2004, doi: 10.1002/pola.11096.

[16] “Chern C-S. Emulsion polymerizations in nonuniform latex particles.Principles and applications of emulsion polymerization. John Wiley & Sons; 2008:200-222”.

[17] “Nicholson J. The chemistry of polymers. Royal Society of Chemistry. 2017”.

[18] Guyot A, “Reactive surfactants in Heterophase polymerization”.

[19] “Reactions And Synthesis In Surfactant Systems”.

[20] “El-hoshoudy A, Desouky S, Betiha M, Alsabagh A. Use of 1-vinyl imidazole based surfmers for preparation of polyacrylamide–SiO 2 nanocomposite through aza-Michael addition copolymerization reaction for rock wettability alteration. Fuel. 2016;170:161-175”.

[21] “Carey V, Wang Y-G. Mixed-effects models in S and S-PLUS. Journal of the American Statistical Association, Taylor & Francis. 2001;(96):1135-1136”.

[22] “Pan ZW, Dai ZR, Wang ZL. Nanobelts of semiconducting oxides. Science. 2001;291(5510): 1947-1949”.

[23] “El-hoshoudy A, Desouky S, Betiha M, Alsabagh A. Use of 1-vinyl imidazole based surfmers for preparation of polyacrylamide–SiO 2 nanocomposite through aza-Michael addition copolymerization reaction for rock wettability alteration. Fuel. 2016;170:161-175”.

[24] “El Hoshoudy A, Desouky S, Al-sabagh A, El-kady M, Betiha M, Mahmoud S. Synthesis and Characterization of Polyacrylamide Crosslinked Copolymer for Enhanced Oil Recovery and Rock Wettability Alteration 2015;3(4):47-59”.

[25] “Li X, Zhu D, Wang X, Wang N, Gao J, Li H. Thermal conductivity enhancement depen- dent pH and chemical surfactant for cu-H 2 O nanofluids. Thermochimica Acta. 2008;469(1):98-103”.

[26] “Reb P, Margarit-Puri K, Klapper M, Müllen K. Polymerizable and nonpolymerizable isophthalic acid derivatives as surfactants in emulsion polymerization. Macromolecules. 2000;33(21):7718-7723”.

[27] “Summers M, Eastoe J. Applications of polymerizable surfactants. Advances in Colloid and Interface Science. 2003;100:137-152”.

[28] “Wang Y, Wu F. Amphiphilic acrylamide-based copolymer with porphyrin pendants for the highly selective detection of hg 2+ in aqueous solutions. Polymer. 2015;56:223-228”.

[29] “Xue W, Hamley IW, Castelletto V, Olmsted PD. Synthesis and characterization of hydro- phobically modified polyacrylamides and some observations on rheological properties. European Polymer Journal. 2004;40(1):47-56”.

[30] “Freedman HH, Mason JP, Medalia A. Polysoaps. II. The preparation of vinyl soaps1. The Journal of Organic Chemistry. 1958;23(1):76-82”.

[31] “Summers M, Eastoe J, Richardson RM. Concentrated polymerized cationic surfactant phases. Langmuir. 2003;19(16):6357-6362”.

[32] “Benbayer C, Saidi-Besbes S, de Givenchy ET, Amigoni S, Guittard F, Derdour A. Copoly merization of novel reactive fluorinated acrylic monomers with styrene: Reactivity ratio determination. Colloid and Polymer Science. 2014;292(7):1711-1717”.

[33] “Samakande A, Hartmann PC, Cloete V, Sanderson RD. Use of acrylic based surfmers for the preparation of exfoliated polystyrene–clay nanocomposites. Polymer. 2007;48(6): 1490-1499”.

[34] “X-J X, Chen F. Semi-continuous emulsion copolymerization of butyl methacrylate with polymerizable anionic surfactants. Polymer. 2004;45(14):4801-4810”.

[35] “Arz C. The use of nonionic polymerizable surfactants in latexes and paints. Macro molecular Symposia. 187. Wiley Online Library; 2002:199-206.”.

[36] “Eliseeva VI, Ivanchev S, Kuchanov S, Lebedev A. Emulsion polymerization and its appli- cations in industry. Springer Science & Business Media; 2012:3-24”.

[37] “Thickett SC, Gilbert RG. Emulsion polymerization: State of the art in kinetics and mecha- nisms. Polymer. 2007;48(24):6965-6991”.

[38] “Yamak HB. Emulsion polymerization: effects of polymerization variables on the proper- ties of vinyl acetate based emulsion polymers. Polymer Science. InTechopen; 2013:35-72”.

[39] “Antonietti M, Tauer K. 90 years of polymer latexes and heterophase polymerization: More vital than ever. Macromolecular Chemistry and Physics. 2003;204(2):207-219”.

[40] “Nucleation and growth in solution synthesis of nanostructures – From fundamentals to advanced applications”.

[41] C. Schick, R. Androsch, and J. W. P. Schmelzer, “Homogeneous crystal nucleation in polymers,” *Journal of Physics Condensed Matter*, vol. 29, no. 45. Institute of Physics Publishing, Oct. 10, 2017. doi: 10.1088/1361-648X/aa7fe0.

[42] Y. U. Long, R. A. Shanks, and Z. H. Stachursilit, “KINETICS OF POLYMER CRYSTALLISATION,” 1995.

[43] C.-S. Chern, “PRINCIPLES AND APPLICATIONS OF EMULSION POLYMERIZATION.”

[44] “C.S. Chern, H.J. Tang Microemulsion polymerization kinetics and mechanisms”.

[45] “Chern CS. Emulsion polymerization mechanisms and kinetics. Progress in Polymer Science. 2006;31(5):443-486”.

[46] H. Wang, Q. Pan, and G. L. Rempel, “Micellar nucleation differential microemulsion polymerization,” *Eur Polym J*, vol. 47, no. 5, pp. 973–980, May 2011, doi: 10.1016/j.eurpolymj.2010.11.009.

[47] “Bauer, K.H., Lehmann, K., Osterwald, H.P., Rothgang, G., 1998. Coated PharmaceuticalDosage Forms. CRC Press, Boca Raton.”.

[48] “V. Granier, A. Sartre, Langmuir 11 (1995) 2179.”.

[49] “R.E. Dillon, E.B. Bradford, R.D. Andrews, Jr.. Ind. Eng. Chem. 45 (1953) 728.”.

[50] “S.S. Voyutskii, J. Polym. Sci. 32 (1958) 528.”.

[51] “T.F. Protzman, G.L. Brown, J. Appl. Polym. Sci. 4 (1960) 81.”.

[52] “ASTM D 2354-68, ‘'Standard Test Method for Minimum Film Formation Temperature (MFT) of Emulsion Vehicles’, American”.

[53] “A van Tent. K. te Nijenhuis, Prog. Org. Coatings 20 (t992) 459.”.

[54] “S.T. Eckersley, A. Rudin, Journ. Coatings Techn. 62 (1990) 89.”.

[55] “M.A. Winnik, Y. Wang, F. Haley, Journ. Coatings Tech. 64 (8i 1) (1992) 51.”.

[56] “J.G. Brodnyan, T. Konen, J. AppI. Polym. Sci. 8 (I964) 687.”.

[57] “R.R. Myers, R.K. Schultz, J. Appl. Polym. Sci. 8 (1964) 755.”.

[58] “D.M.C. Heymans, M.F. Daniel, Polym. Adv. Techn. 6 (1995) 291.”.

[59] “S.T. Eckersley, A. Rudin, J. Appl. Polym. Sci. 48 (1993) 1369”.

[60] J. T. P. Derksen, F. P. Cuperus, and P. Kolster, “Renewable resources in coatings technology: a review,” 1996.

[61] G. Lligadas, J. C. Ronda, M. Galià, and V. Cádiz, “Renewable polymeric materials from vegetable oils: A perspective,” *Materials Today*, vol. 16, no. 9. pp. 337–343, Sep. 2013. doi: 10.1016/j.mattod.2013.08.016.

[62] R. L. Quirino, K. Monroe, C. H. Fleischer, E. Biswas, and M. R. Kessler, “Thermosetting polymers from renewable sources,” *Polym Int*, vol. 70, no. 2, pp. 167–180, Feb. 2021, doi: 10.1002/pi.6132.

[63] “Feedstocks for the Future: Renewable for the Pro- duction of Chemicals and Materials; Bozell, J. J.; Patel, M., Eds.; ACS Symposium Series 921; American Chemical Society: Washington, DC, 2006.”.

[64] C. Zhang, T. F. Garrison, S. A. Madbouly, and M. R. Kessler, “Recent advances in vegetable oil-based polymers and their composites,” *Prog Polym Sci*, vol. 71, pp. 91–143, Aug. 2017, doi: 10.1016/J.PROGPOLYMSCI.2016.12.009.

[65] G. R. Ferreira, J. R. Braquehais, W. N. da Silva, and F. Machado, “Synthesis of soybean oil-based polymer lattices via emulsion polymerization process,” *Ind Crops Prod*, vol. 65, pp. 14–20, Mar. 2015, doi: 10.1016/j.indcrop.2014.11.042.

[66] L. S. Laurentino, A. M. M. S. Medeiros, F. Machado, C. Costa, P. H. H. Araújo, and C. Sayer, “Synthesis of a biobased monomer derived from castor oil and copolymerization in aqueous medium,” *Chemical Engineering Research and Design*, vol. 137, pp. 213–220, Sep. 2018, doi: 10.1016/j.cherd.2018.07.014.

[67] S. K. Sahoo, V. Khandelwal, and G. Manik, “Synthesis and characterization of low viscous and highly acrylated epoxidized methyl ester based green adhesives derived

from linseed oil," *Int J Adhes Adhes*, vol. 89, pp. 174–177, Mar. 2019, doi: 10.1016/j.ijadhadh.2019.01.007.

[68] "Advances in the Research and Development of Acrylic Acid Production from Biomass*."

[69] A. J. J. Straathof, S. Sie, T. T. Franco, and L. A. M. Van Der Wielen, "Feasibility of acrylic acid production by fermentation," *Applied Microbiology and Biotechnology*, vol. 67, no. 6. pp. 727–734, Jun. 2005. doi: 10.1007/s00253-005-1942-1.

[70] C. Gao, C. Ma, and P. Xu, "Biotechnological routes based on lactic acid production from biomass," *Biotechnology Advances*, vol. 29, no. 6. pp. 930–939, Nov. 2011. doi: 10.1016/j.biotechadv.2011.07.022.

[71] T. Dishisha, S. H. Pyo, and R. Hatti-Kaul, "Bio-based 3-hydroxypropionic- and acrylic acid production from biodiesel glycerol via integrated microbial and chemical catalysis," *Microb Cell Fact*, vol. 14, no. 1, Dec. 2015, doi: 10.1186/s12934-015-0388-0.

[72] L. Cao, J. Wang, C. Liu, Y. Chen, K. Liu, and S. Han, "Ethylene vinyl acetate copolymer: A bio-based cold flow improver for waste cooking oil derived biodiesel blends," *Appl Energy*, vol. 132, pp. 163–167, Nov. 2014, doi: 10.1016/j.apenergy.2014.06.085.

[73] A. Djukić-Vuković, D. Mladenović, J. Ivanović, J. Pejin, and L. Mojović, "Towards sustainability of lactic acid and poly-lactic acid polymers production," *Renewable and Sustainable Energy Reviews*, vol. 108, pp. 238–252, Jul. 2019, doi: 10.1016/j.rser.2019.03.050.

[74] F. S. Fattahi, A. Khoddami, and O. Avinc, "Sustainable, Renewable, and Biodegradable Poly(Lactic Acid) Fibers and Their Latest Developments in the Last Decade," 2020, pp. 173–194. doi: 10.1007/978-3-030-38013-7_9.

[75] H. Ramezani Dana and F. Ebrahimi, "Synthesis, properties, and applications of polylactic <scp>acid-based</scp> polymers," *Polym Eng Sci*, vol. 63, no. 1, pp. 22–43, Jan. 2023, doi: 10.1002/pen.26193.

[76] A. Kohut *et al.*, “Emulsion Polymerization of Plant Oil-Based Acrylic Monomers: Resourceful Platform for Biobased Waterborne Materials,” 2020, pp. 27–66. doi: 10.1021/bk-2020-1372.ch003.

[77] M. Kolář, J. Machotová, M. Hájek, J. Honzíček, T. Hájek, and Š. Podzimek, “Application of Vegetable Oil-Based Monomers in the Synthesis of Acrylic Latexes via Emulsion Polymerization,” *Coatings*, vol. 13, no. 2, Feb. 2023, doi: 10.3390/coatings13020262.

[78] P. Cognard, “Equipment for the Application of Adhesives and Sealants: Mixing, Metering, Coating or Applying the Adhesives,” 2006, pp. 51–xxxvii. doi: 10.1016/S1874-5695(06)80013-8.

[79] H. Ling and L. Junyan, “Synthesis, modification and characterization of core–shell fluoroacrylate copolymer latexes,” *J Fluor Chem*, vol. 129, no. 7, pp. 590–597, Jul. 2008, doi: 10.1016/j.jfluchem.2008.04.007.

[80] K. Matyjaszewski and T. P. Davis, Eds., *Handbook of Radical Polymerization*. Wiley, 2002. doi: 10.1002/0471220450.

[81] P. A. Steward, J. Hearn, and M. C. Wilkinson, “An overview of polymer latex film formation and properties,” 2000.

[82] C. J. Brinker, P. R. Schunk, G. C. Frye, and C. S. Ashley, “NON-CRYSTALLINE SOLIDS Review of sol-gel thin film formation,” 1992.

[83] “ ISO 22412:2017. Particle Size Analysis – Dynamic Light Scattering (DLS). International Organization for Standardization”.

[84] “CHR6. Zeta Potential Measurements-Zeta Theory. In: NanoComposix [online].©2020nanoComposix [cit. 2019-10-29].”.

[85] “Heat Flux DSC [schematic]. In: Research and Reviews-International Journals Research & Reviews: Journal of Pharmaceutical Analysis Search here.: Differential Scanning Calorimetry: A Review [online]. Copyright © 2020Research and Reviews[feeling. 2019-10-29]. ”.

[86] “Heat Flux DSC [schematic]. In: Research and Reviews-International Journals Research & Reviews: Journal of Pharmaceutical Analysis Search here.: Differential Scanning Calorimetry: A Review [online]. Copyright © 2020Research and Reviews[feeling. 2019-10-29]. ”.